



International Summer School
Stellar Winds and Outflows

3.–15. September 2023, Harrachov, Czech Republic

Overview of Stellar Winds and Outflows

Olga Maryeva and Lydia Cidale

Stellar Outflows: basic terminology

Stellar outflows are streams of particles, such as gas and dust, expelled from a star's surface. They are observed at all stages of the Main-sequence and post-Main sequence evolution.

Types of Outflows



Stellar wind is the continuous, supersonic outflow of matter from the surface layers of a star. It consists of **streams of charged particles**, primarily **electrons and protons**. These particles achieve enough energy to overcome the star's gravitational field and escape into space.

High resolution images reveal outflows and their interaction with the surroundings

Protostellar Outflows: These outflows are observed during the **formation of the stars**. They are driven by the interaction between the infalling material and the strong magnetic fields near the young star.

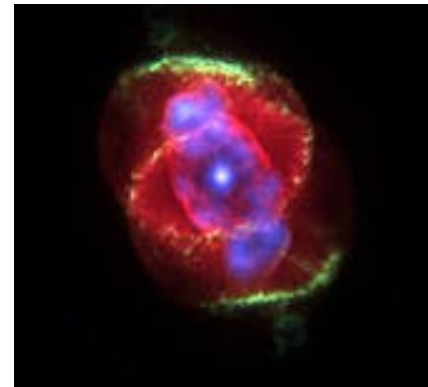


Types of Outflows: basic terminology

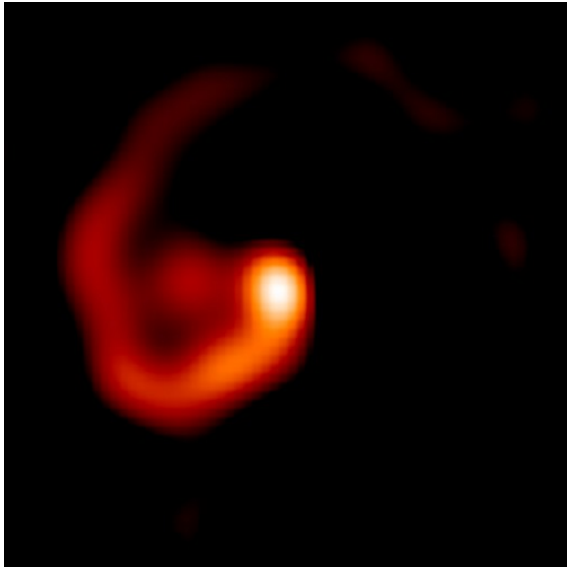
Post-Main-Sequence Outflows: As stars evolve into (or back from) red giants or supergiants, they can shed their outer layers through strong winds.

High-mass stars: OB supergiants, WR stars, Luminous Blue Variables, B[e] stars show **strong winds** with P Cygni profiles. Many of them have spatially resolved circumstellar shells that are fossils of previous eruptions.

Low- to intermediate-mass stars also lose a **significant amount of mass** through stellar winds or more violent and recurrent processes like planetary nebula ejections.



Types of Outflows: basic terminology



Accretion Disk Outflows: In binary systems or around young stars, material can accrete onto a central object (such as a white dwarf, neutron star, or black hole). Some of this accreted material may be ejected in the form of powerful and dusty outflows.

The influence of binaries on the observed distribution of massive stars comes through the process of mass loss and mass transfer via Roche-lobe overflow (RLOF). Sometimes, they show dynamical events.

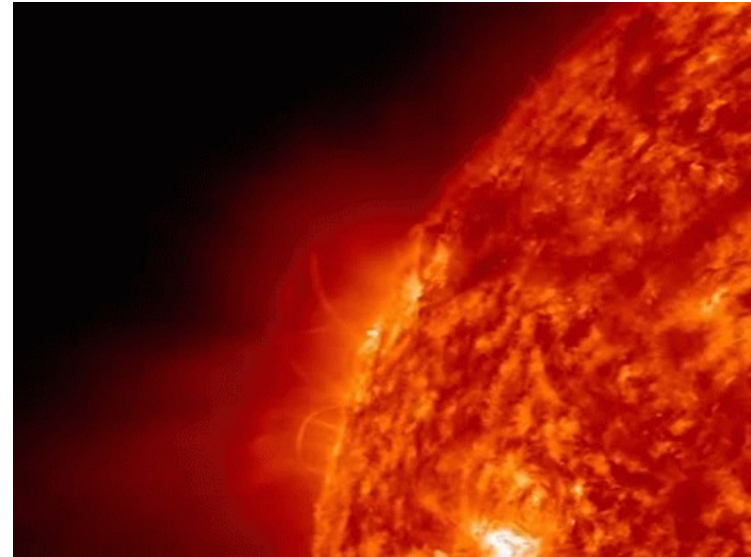
WR 98A → Astrophysical Journal Letters 1999, 525, L97 - Pinwheel shapes

Outburst: basic terminology

Outburst are associated with various stages of a star's life cycle and can have significant effects on their surroundings

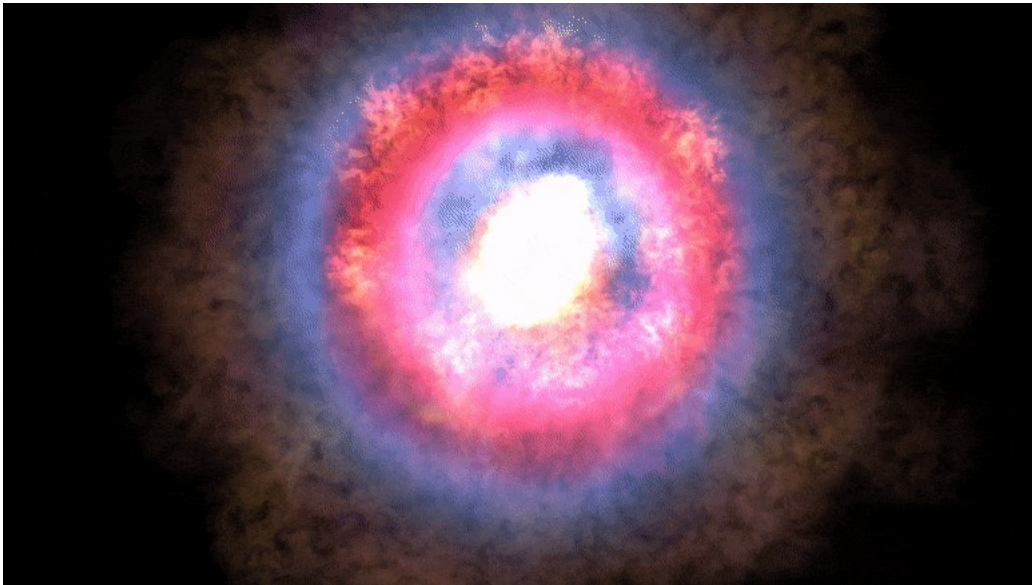
Category: **Novae, Supernovae, Supernova impostors & Stellar flares**

- Interactions between binary star systems with eccentric orbits (X-Ray outbursts)
- Instabilities in the star's interior
- Flares and Coronal mass ejections (CME).



The History of Stellar Winds & Outflows

The **concept of stellar winds** can be traced back to the earliest sky observations via brief eruptive events



SN 1572: “Tycho Brahe’s remnant was the first evidence showing that change occurred beyond the Earth’s atmosphere and against the Aristotelian cosmological views.”

B Cassiopeiae (B Cas)

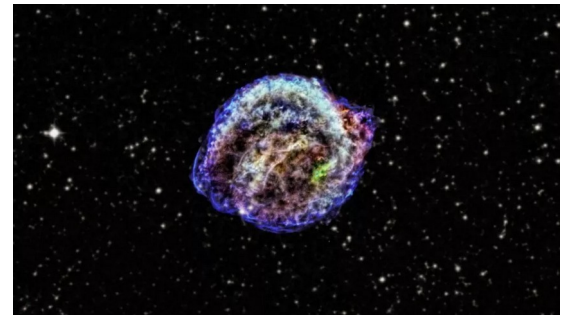
Early Interpretation of Stellar Outflows

Only seven supernovae are known to have been recorded before the early 17th century.

- **“Nova stars”** (supernova explosions). First recorder of supernova explosion (RCW 86). On December 7th, 185 AD, 2nd year of the Chung-ping reign period



- **1054 - The Crab Nebula**
Chinese astronomers reported a new star. The Crab Nebula supernova remnant and pulsar wind nebulae in Taurus. The nebula was discovered by J. Bevis in 1731



- **1604 - The Kepler's supernova remnant**

Image observed with NASA's Chandra X-ray Observatory (Image credit: X-ray: NASA/CXC/NCSU/M.Burkey et al; Optical: DSS)

Early Observations of Stellar Outflows



- In 1600, Willem Blaeu reported the outburst of the P Cygni star (LBV), on a globe made by himself, now in a Prague museum: "The new star in Cygnus that I first observed on 8 August 1600, was initially of third magnitude". The star showed magnitude fluctuations until 1759.



Spectrum of Sun



Spectrum of WR 137
(one of Wolf and Rayet's prototypes in Cygnus)



"Great Eruption" of Eta Carina was in 1837
fading well below [naked-eye](#) visibility after 1856.
Small eruptions were later detected.

The homunculus was discovered in 1950 by E.
Gaviola (Bosque Alegre, Córdoba, Argentina)
[Fe II] lines in absorption → Tackeray (1953)

- Based on spectroscopic studies, "peculiar bright lines" were discovered by Wolf & Rayet (1867) (WR stars).
- The Pickering Series (now He lines)

Early Interpretation of Solar Outflows

- ☐ **Comets' tails:** In the 17th century, J. Kepler and C. Huygens proposed that the tails of comets were formed by a **force from the Sun**, which could be considered the beginning of **stellar wind theory**.



- ☐ **Northern lights:** Carrington Event, Solar eruptions (Flares) 1 September 1859 while observing sun spots.



History of Studies: From Nova to P Cygni profiles

Late 19th and early 20th century

Campbell 1892-1894 performed first spectroscopic observations of a Nova

Nova Aurigae flashed in 1891

The spectra changed from hour to hour from night to night.

The width of line was proportional to the wavelength → Doppler effects produced broadening

Barnard (1918) measured the angular ring of **Nova Aquilae**. Detected for months after maximum a feature with a diameter of $2''$ of arc. The expansion continued uniformly until 1941, that became to faint. He measured a radial velocity of 1600 km s^{-1}

Doppler effect

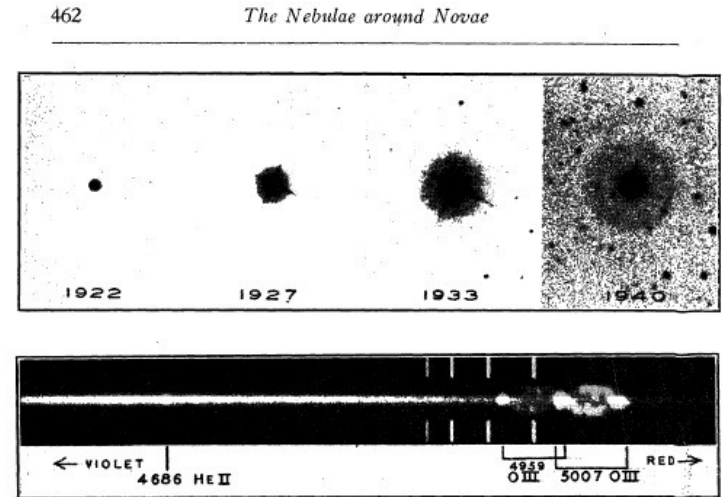


FIGURE 1

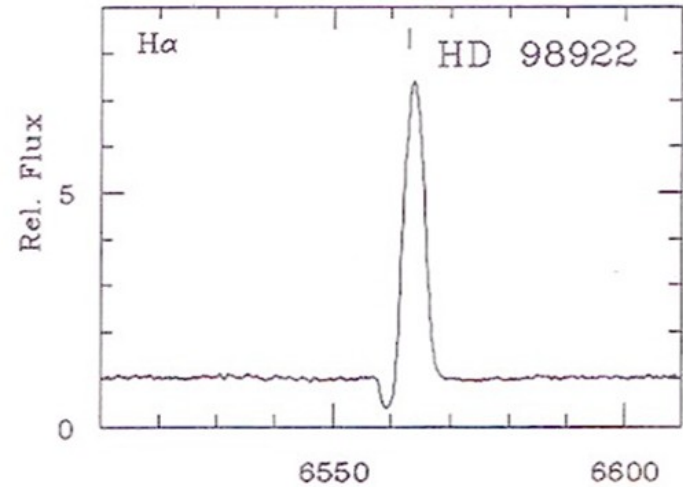
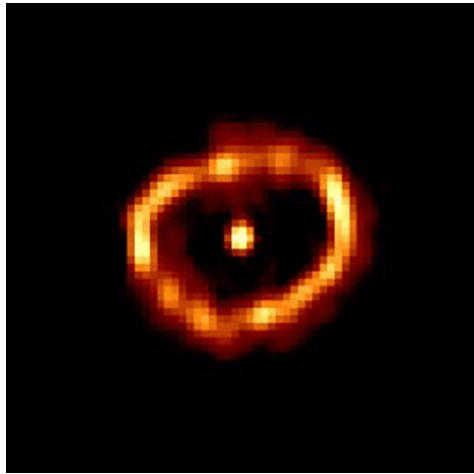
Courtesy of *Sky and Telescope*

Top: The expanding nebula around Nova Aquilae 1918, taken at Mount Wilson. These are negatives. The central strong spot is the much-overexposed image of the star; the four rays are due to light diffraction by the secondary mirror supports.

Below: The spectrum of Nova Aquilae and its expanding nebular shell, photographed with iron comparison lines at Mount Wilson in July, 1920, with a much greater scale than in the direct photographs above. The horizontal streak is the star's spectrum, continuous except for the bright knot 4686 of ionized helium. At the right are two Doppler ellipses of doubly ionized oxygen in the nebula.

History of Studies: From Nova to P Cygni profiles

P Cygni line profile as evidence of expanding shells



Campbell suggested the link

History of Studies: Evolution of Nova Envelopes

Nova GK Per

Liimets et al. (2012)



1953

GK Persei (also **Nova Persei 1901**) was a bright nova discovered by T. Anderson.

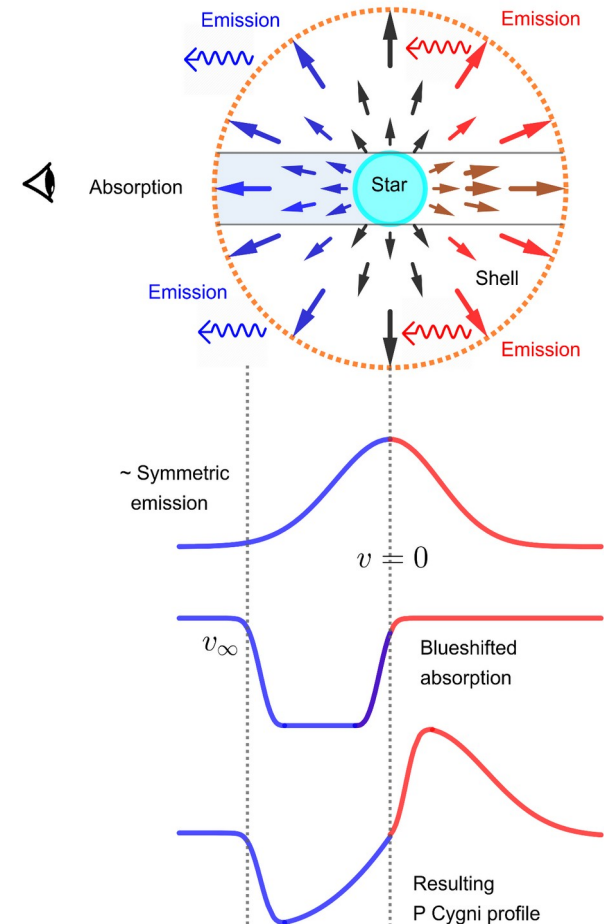
It is a close binary system (cataclysmic variable)

History of Studies: Interpretation of P Cygni profiles

Spectrum of Nova Ophiuchi

Adams & Burwell (1920) concluded “The Doppler effect is the principal agent involved and lends some support to the hypothesis of a shell of gas moving rapidly out from each star.

“A comparison of the widths of the bands in these stars shows that their ratio is closely the same as that between the displacements of the absorption lines, and that in each case the width is very nearly twice that of the corresponding displacement”.



History of Studies: First ideas on line-driven winds

- **Saha (1919)** first idea that atoms can be pushed by absorption of radiation
- **Milne (1924)** and **Johnson (1925)** developed the basic equations for acceleration of matter by **line radiation**, and they suggested that radiation pressure could extend and heat the outer layers of the solar atmosphere.
- **Milne (1926)** highlighted the **Doppler effect** as an important ingredient for the line radiative acceleration. **The force acting** on selected ions due to absorption of photons can exceed gravity and ions then can leave the surface of the star

Momentum and Energy Transfer by Absorption and Scattering

When an atom absorbs and re-emits photons, there is a transfer of momentum and energy from radiation to the medium.

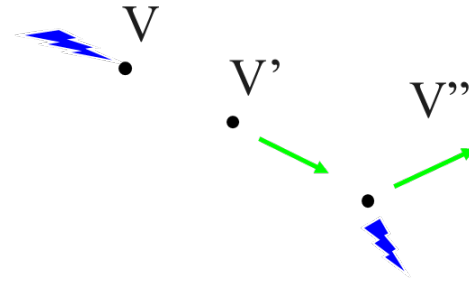
$$mv_r' = mv_r + \frac{h\nu}{c} \quad \Delta v_r = h\nu/mc.$$

If the atom emits a photon ν' at an angle α the new radial velocity is

$$mv_r'' = mv_r' - \frac{h\nu'}{c} \cos \alpha$$

For an external observer,

- The absorbed frequency is $\nu_0 (1 + v_r/c)$
- The emitted frequency is $\nu_0 (1 + v_r'/c)$



The net velocity after absorbing and re-emitting is

$$\begin{aligned}v_r'' &= v_r + \frac{h\nu_0}{mc} \left(1 + \frac{v_r}{c}\right) - \frac{h\nu_0}{mc} \left(1 + \frac{v_r'}{c}\right) \cos \alpha \\ &= v_r + \frac{h\nu_0}{mc} \left(1 + \frac{v_r}{c}\right) (1 - \cos \alpha) - \frac{1}{c} \left(\frac{h\nu_0}{mc}\right)^2 \left(1 + \frac{v_r}{c}\right) \cos \alpha\end{aligned}$$

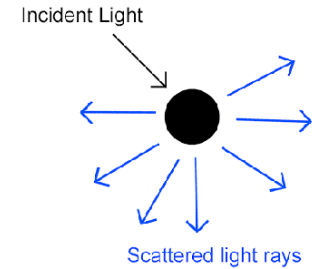
For $v \ll c$ and $h\nu_0 \ll mc$ we find that the radial velocity component of the atom has increased by

$$v_r'' - v_r = \frac{h\nu_0}{mc} (1 - \cos \alpha)$$

- For forward scattering ($\cos \alpha = 1$) $\rightarrow \Delta v = 0$
- For backward scattering ($\cos \alpha = -1$) $\rightarrow \Delta v = 2h\nu_0/c$

For random re-emission of photons, the mean transfer of momentum after the scattering of photons coming in the radial direction is

$$\langle \Delta mv \rangle = \frac{h\nu_0}{c} \frac{1}{4\pi} \int_{-\pi/2}^{\pi/2} (1 - \cos \alpha) 2\pi \sin \alpha d\alpha = \frac{h\nu_0}{c}$$



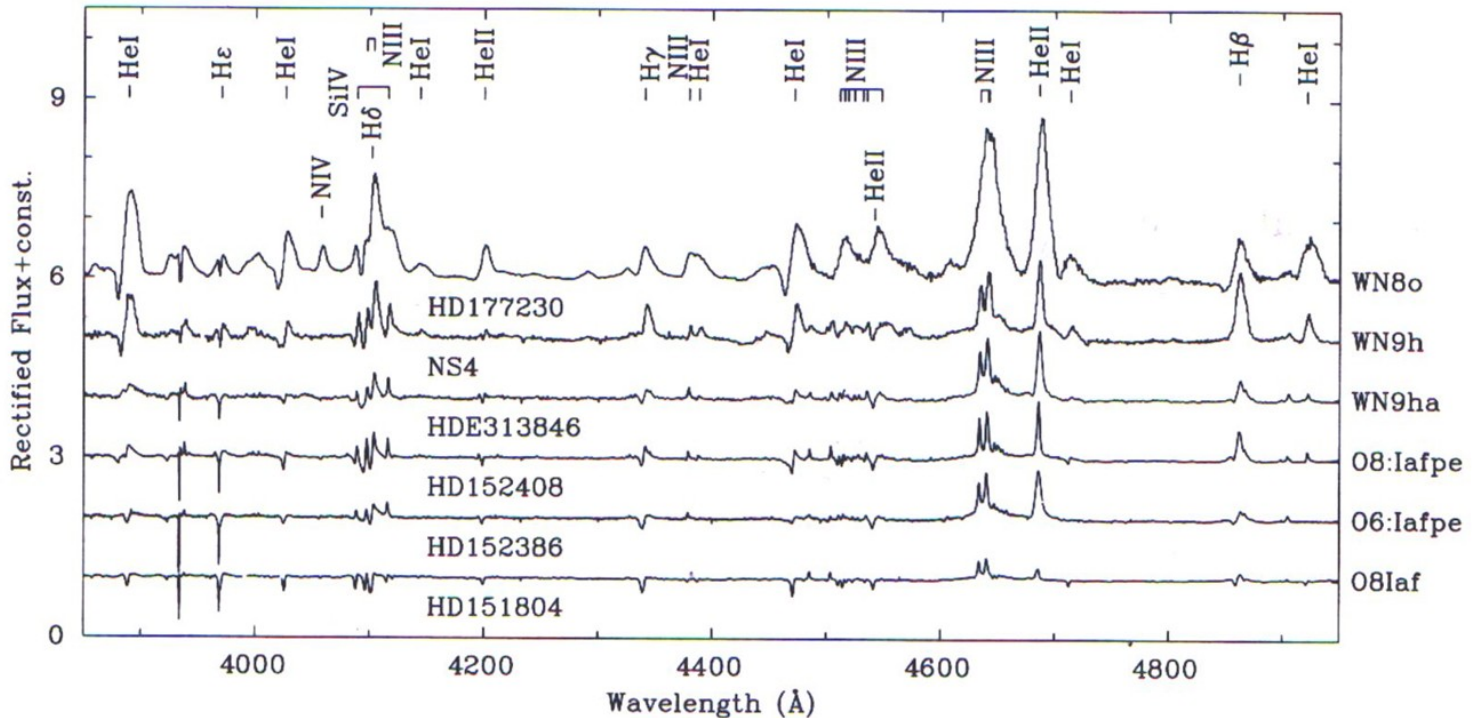
If the absorbed photons were coming from in all directions, the net momentum would be zero

$$\lambda = 765 \text{ \AA} \rightarrow h\nu_0/mc = 37 \text{ cm s}^{-1}$$

- To accelerate N IV ions to 2000 km s^{-1} , we need 10^6 absorption

History of Studies: Wolf-Rayet stars

Beals (1929) suggested WR stars have a “continuous outflow” in radial direction and high velocity due to presence of P Cygni profiles



History of Studies: Pioneering Estimates of Mass Loss Rate

- Kosirev (1934) used radiative transfer theory (Chandrasekhar 1934) to estimate mass-loss rates from observational data.

Wolf-Rayet stars → $10^{-5} M_{\odot} \text{ yr}^{-1}$ and terminal velocities ~ 1000 km s^{-1}

- Adams & Mac Cormack (1935) tiny line shifts ~ 5 km s^{-1}
- Spitzer(1939) proposed the “fountain model” for cool supergiants
- Deutsch (1956) – Cool stars, red giant **binaries** (alpha Her G5+M5) with circumbinary envelope → low terminal velocities and a large mass-loss rate

M giants → $10^{-7} M_{\odot} \text{ yr}^{-1}$

For massive stars, winds remove more than half of the star original mass

History of Studies: Development of stellar winds models

1920's → the foundation of the theory of monochromatic scattering (Eddington, Milne, etc)

1930 - 1960 → accurate approximate solutions to the basic radiative transfer equations (Ambartsumian, Sobolev, Chandrasekhar) for moving media

1958 - 1960 → Theory and observations of the solar wind started in 1958 with the theoretical works of L. Biermann (1946) and E. Parker (1958, 1960) (winds driven by gas pressure gradients)

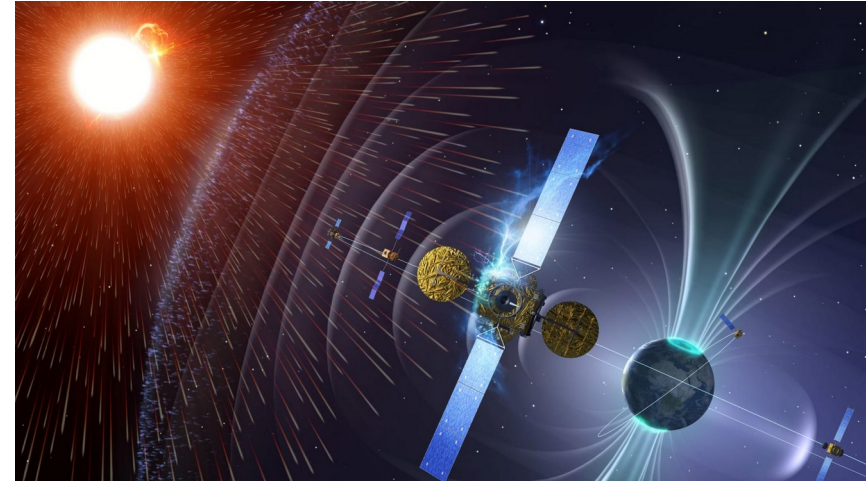
History of Studies: Space Studies of Solar wind

1959 Soviet spacecraft **Luna-1** first directly observed the solar wind and measured its strength using hemispherical ion traps. Next Luna-2 and Luna-3 verified it.

1962 American spacecraft **Mariner-2** showed existence of a constant outflow of plasma from the Sun

late 1990-s SOHO found that the wind accelerates much faster than may be accounted for by thermodynamic expansion alone (**Alfvén waves**)

The first concrete evidence of stellar winds was obtained in 1962.



Average characteristics of solar wind at Earth's orbit:

Velocity 400 km/s

Proton density 6 cm^{-3}

Proton temperature $5 \cdot 10^4 \text{ K}$

Electron temperature $1.5 \cdot 10^5 \text{ K}$

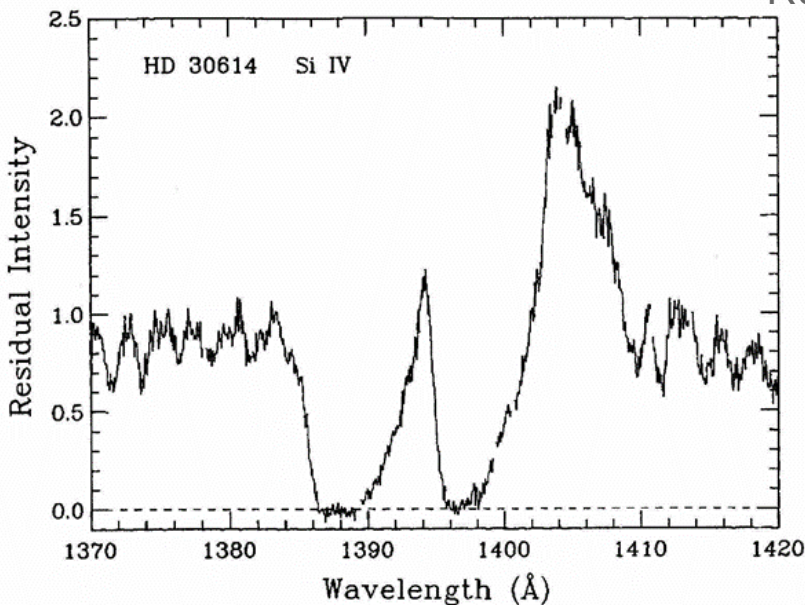
Magnetic field strength $5 \cdot 10^5 \text{ Oe}$

Proton flux density $2.4 \cdot 10^8 \text{ cm}^{-2}\text{s}^{-1}$

Kinetic energy flux density $0.3 \text{ erg} \cdot \text{cm}^{-2}\text{s}^{-1}$

History of Studies: UV spectroscopic observations of massive stars

In the 1970s and 1980s, satellite missions like the Copernicus & International Ultraviolet Explorer (IUE) allowed for the detailed study of stellar ultraviolet spectra, providing the **decisive evidence that all luminous hot stars have strong winds**



Resonance lines of highly ionised elements **Si IV, CIV, N V**

Wind terminal velocities $\sim 1000\text{-}3000 \text{ km s}^{-1}$

- Morton (1967) Ap J 147,1017 - the estimated mass loss **$10^{-6} \text{ Mo yr}^{-1}$**
- Deutsch (1968) confirmed that mass-loss is present across the HR diagram
- Lamers & Morton (1976) Ap. J. Sup. 32, 715

History of Studies: Improved Models of Stellar Winds

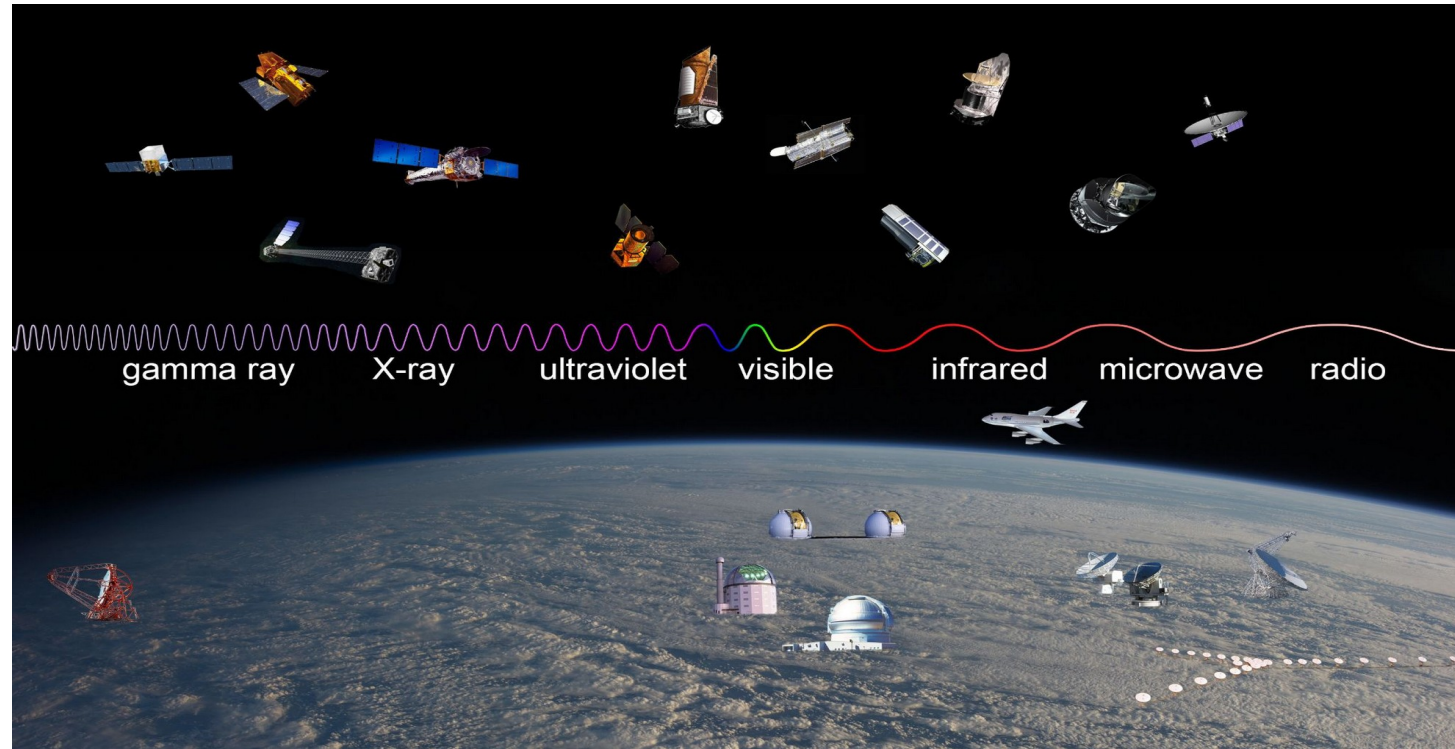
1965 - 1970 → E. Parker developed the Alfvén wave driven wind theory
Weber & Davis (1967) formulated the co-rotating magnetic rotator model

1960 -1990 → Improved solutions for static and moving media. Lucy & Solomon(1970) and Castor, Abbot & Klein (1975) developed the basic equations of line-driven winds.

1970 - The development of IR detectors led to a similar recognition of the importance of dust-driven winds in RSGs (Gehrz & Woolf 1971)

Today → Computational hydrodynamical simulations and radiative transfer codes have become more sophisticated (2D and 3D models)

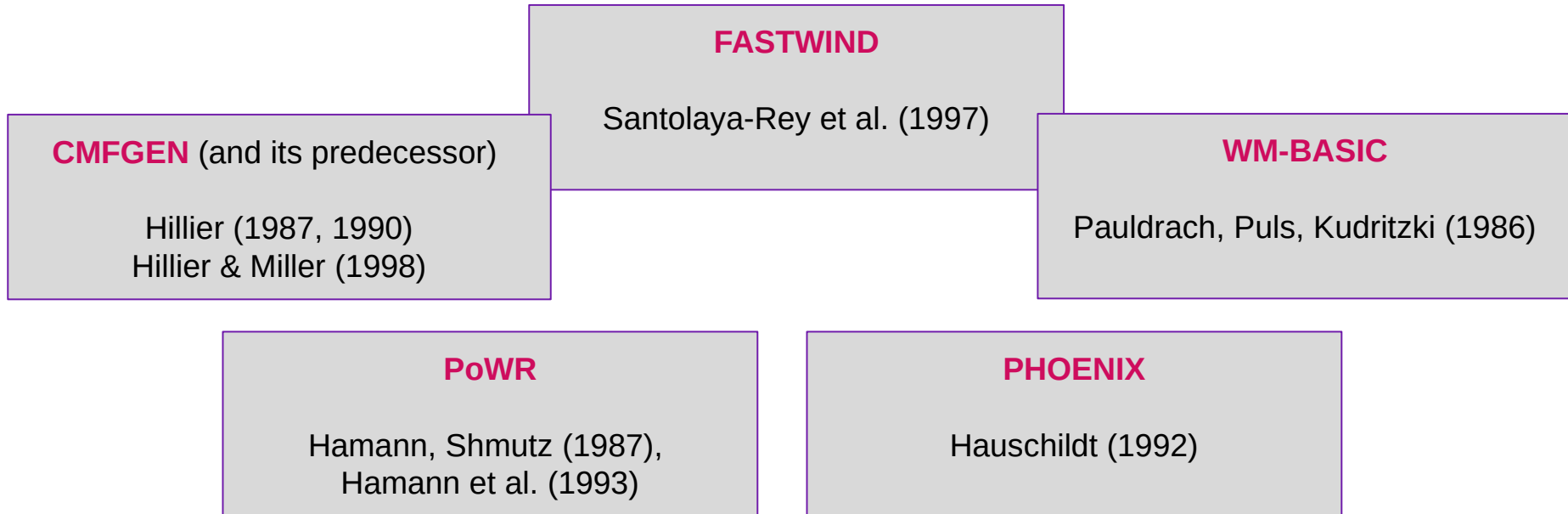
History of Studies: Satellites give our today view of outflows



History of Studies: Development of Numerical Methods

Mihalas, Kunasz, and Hummer (1975) presented a method for solving the line-formation problem using full comoving-frame formulation of the radiative-transfer equation for the case of spherically symmetric atmospheres expanding with arbitrarily large velocities. It initiated the development of numerical modeling methods and codes.

Hauschildt (1992) – fast method for the solution of the radiative transfer equation in rapidly moving spherical media, based on an approximate Λ -operator iteration



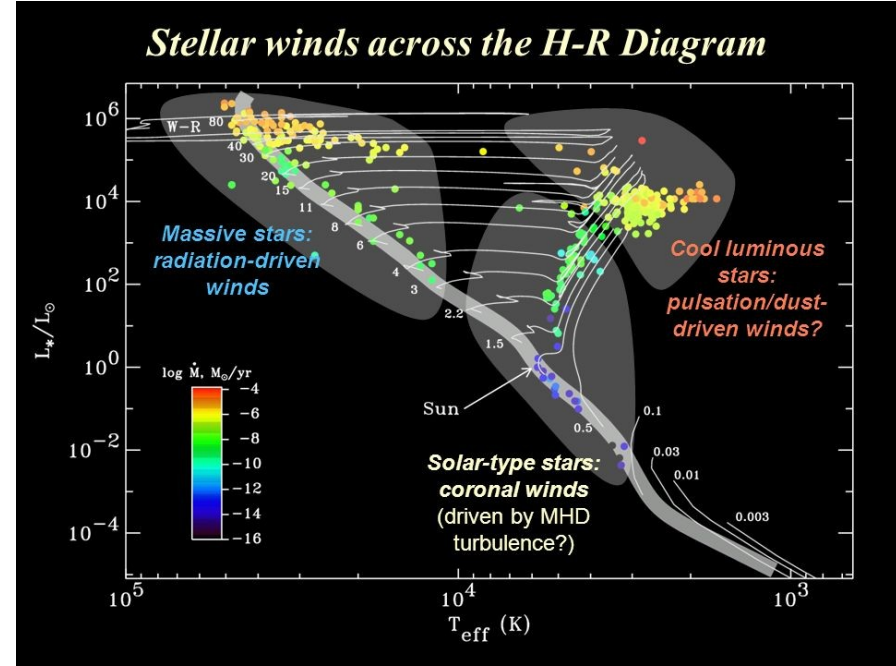
Properties of stars along the HR diagram

Massive stars

- Bipolar magnetic fields
- Radiative atmospheres
- Radiation driven winds
- High rotators
- Pulsations

Solar-type stars

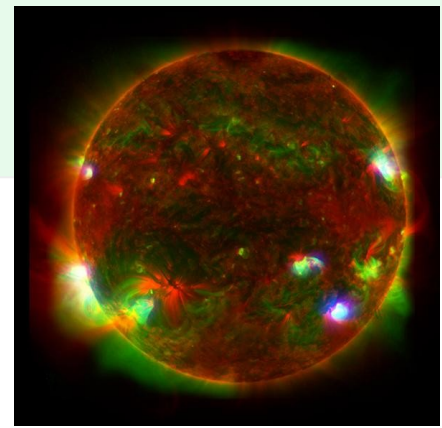
- Slow rotators
- Corona
- Convective atmospheres
- Thermal winds (corona)
- Multipolar magnetic fields



Main mechanisms responsible for Stellar Winds

- **Radiation Pressure:** Stars emit intense radiation. This radiation exerts pressure on the star's outer layers, leading to material expulsion.
- **Gas Pressure:** The outer layers of stars (**corona**) are heated to high temperatures. Particles gain kinetic energy and escape from the star's gravitational field.
- **Magnetic fields:** magnetic fields can channel and accelerate particles that can escape from the star's gravitational field.
- **Coronal Mass Ejections (CMEs)** are sudden and violent releases of plasma and magnetic fields from a star's corona. CMEs can carry a significant amount of material into space at high speeds
- **Sound waves and Alfvén waves** in the atmospheres of cool stars create wave pressure
- **Pulsations** cause a periodic buildup of radiative energy in the stellar interior that is released suddenly

Solar-type stars: Coronal Winds

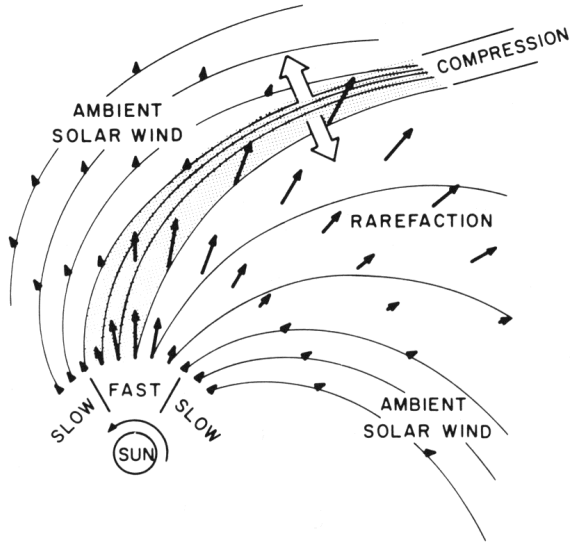


- The solar wind is driven by the gas-pressure gradient of the high-temperature solar corona
- Corona, heated by mechanical energy generated in the solar convection zone, is main reason for gas-pressure appearance
- Magnetic fields lead to extensive structure and variability in the solar corona and wind

$$\dot{M} = (2-3) \times 10^{-14} M_{\odot} \text{ year}^{-1}$$

Fast solar wind originates from coronal holes

Cool stars ($T_{\text{surf}} \lesssim 10000$) should have vigorous subsurface convection zones that generate a strong upward flux of mechanical energy. Observations of X-ray emission and high-ionization UV lines do indeed provide strong evidence for such stellar coronae, but very low mass loss rate means there are few direct diagnostics of actual outflow in stellar coronal winds



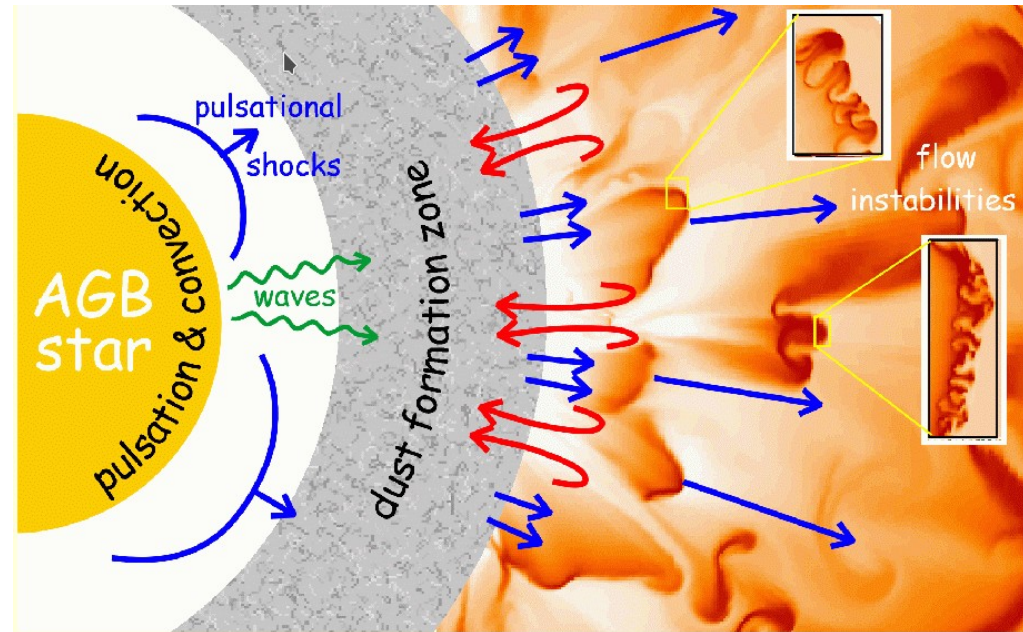
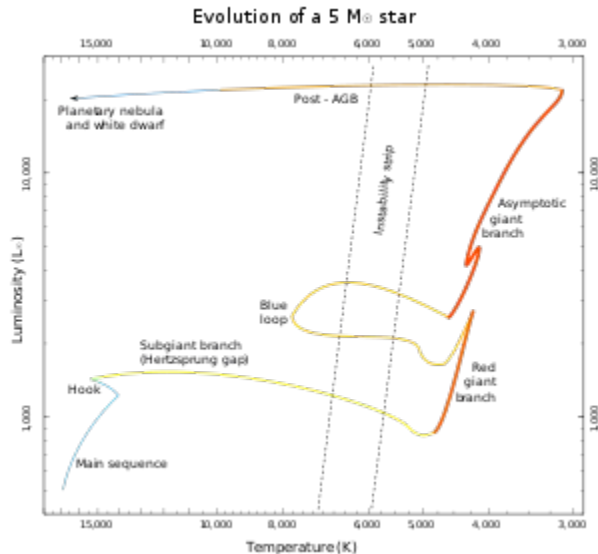
Asymptotic Giant Branch: Pulsations

Stellar pulsations, perhaps augmented by radiative scattering on dust, can apparently induce a much stronger, even runaway mass loss.

Thermal pulses produce periods of even higher mass loss and may result in detached shells of circumstellar material. A star may lose 50 to 70% of its mass during the AGB phase.

$$\dot{M} = 10^{-8} \text{ to } 10^{-5} M_{\odot} \text{ year}^{-1}$$

$$\text{upto } 10^{-4} M_{\odot} \text{ year}^{-1}$$



Sound Wave Driven Winds

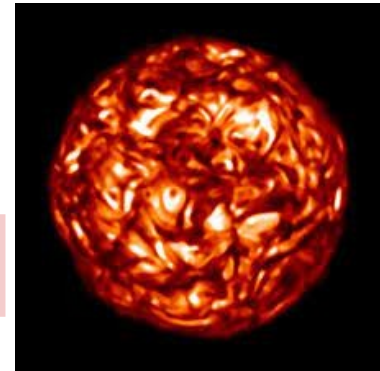
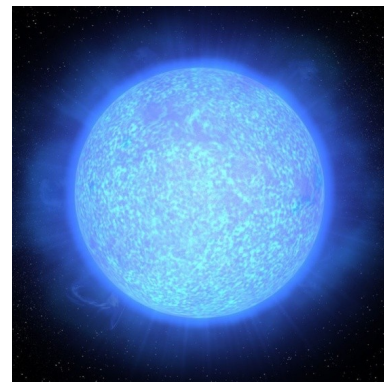
In stars with a convective zone just below the photosphere, the convective motion might create acoustic waves which propagate outwards through the photosphere. These sound-waves produce additional pressure, “wave pressure”, in the atmosphere. This pressure will depend on the density and amplitudes of the waves. The wave pressure gradient creates a force that can cause a stellar wind. If the stellar wind is driven by acoustic waves pressure, then it is called “sound wave driven wind”.



Acoustic waves pressure important only in cool low mass stars – Asymptotic Giant Branch (AGB) – but pulsation is more important than acoustic waves for driving the winds of AGB stars

Radiation Driven Winds

The outer atmospheres of luminous cool giant stars and early-type stars can be driven outward by the strong radiation fields from the stellar photospheres.



Radiation Driven Winds

Line Driven

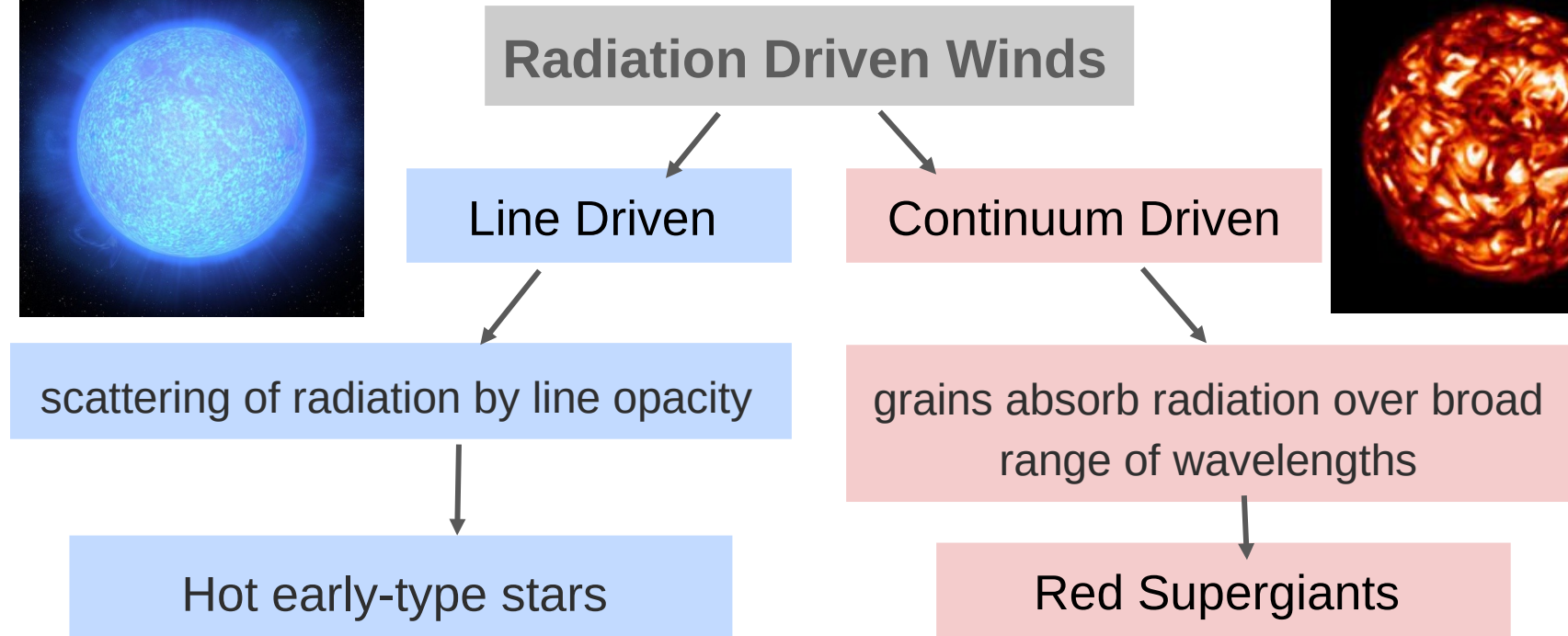
Continuum Driven

scattering of radiation by line opacity

grains absorb radiation over broad range of wavelengths

Hot early-type stars

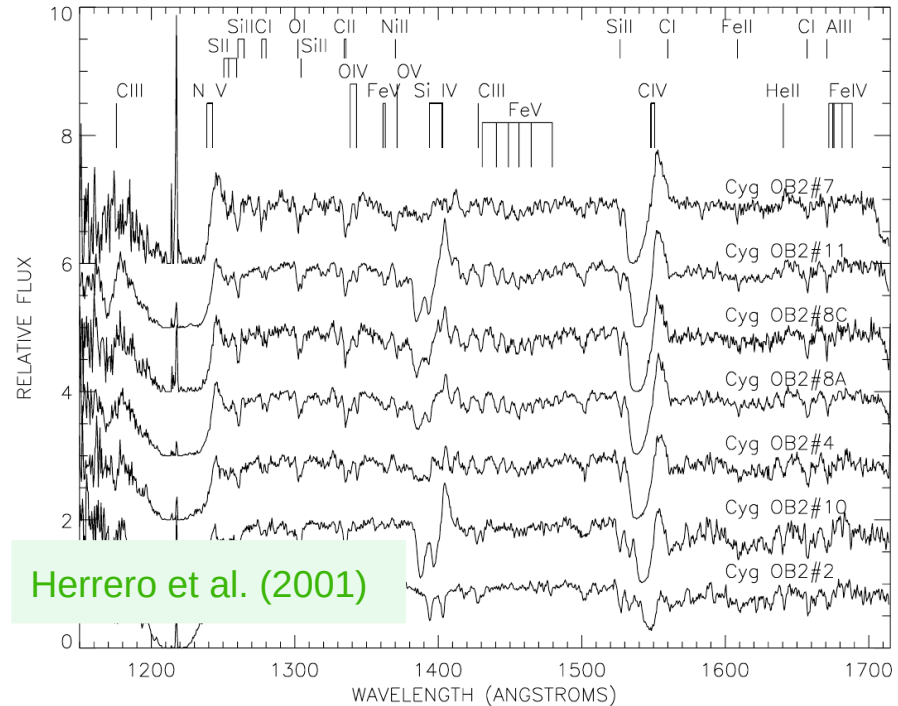
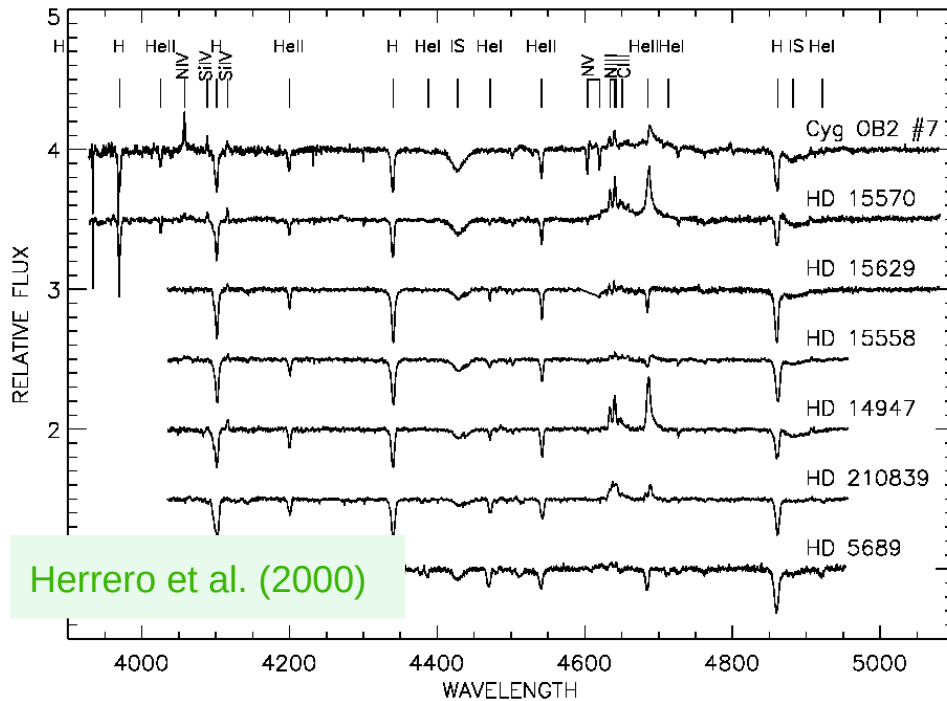
Red Supergiants



Hot Massive Stars: Line Driven Winds

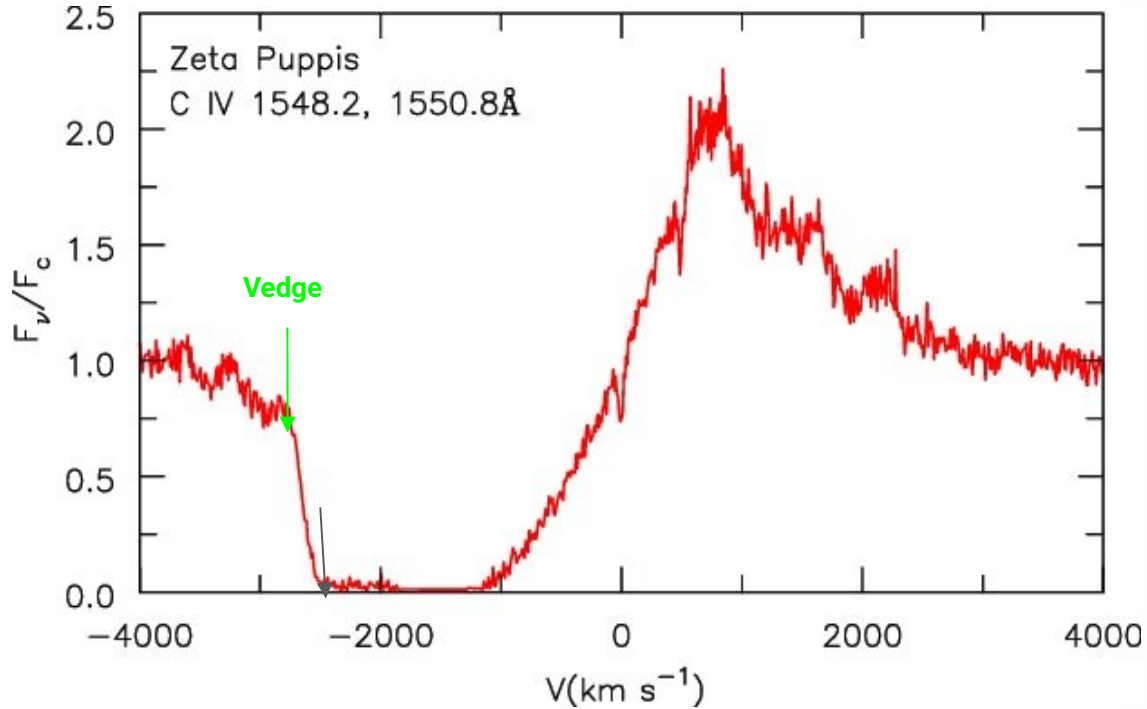
$$L_l = \frac{1}{8\pi R_*} \left(\frac{\dot{M}}{v_\infty} \right)^2 \int_{x_{min}}^{\infty} \frac{f_{rec}(T)}{wx^2} \left\{ 1 - \sqrt{1 - (x_{min}/x)^2} \right\} dx; \quad \dot{M} \sim v_\infty \sqrt{L_l}$$

For OB-type stars luminosity in the line is accurate indicator of mass loss rate if the terminal velocity is measured from P Cygni profiles in the ultraviolet range



Determination of the Terminal Velocity

Saturated resonance-line UV profiles for estimation V_{∞}



The C IV P Cygni profile in the O4 I(n)fp star Zeta Puppis. Terminal velocity $V_{\infty} \sim 2600 \text{ km s}^{-1}$

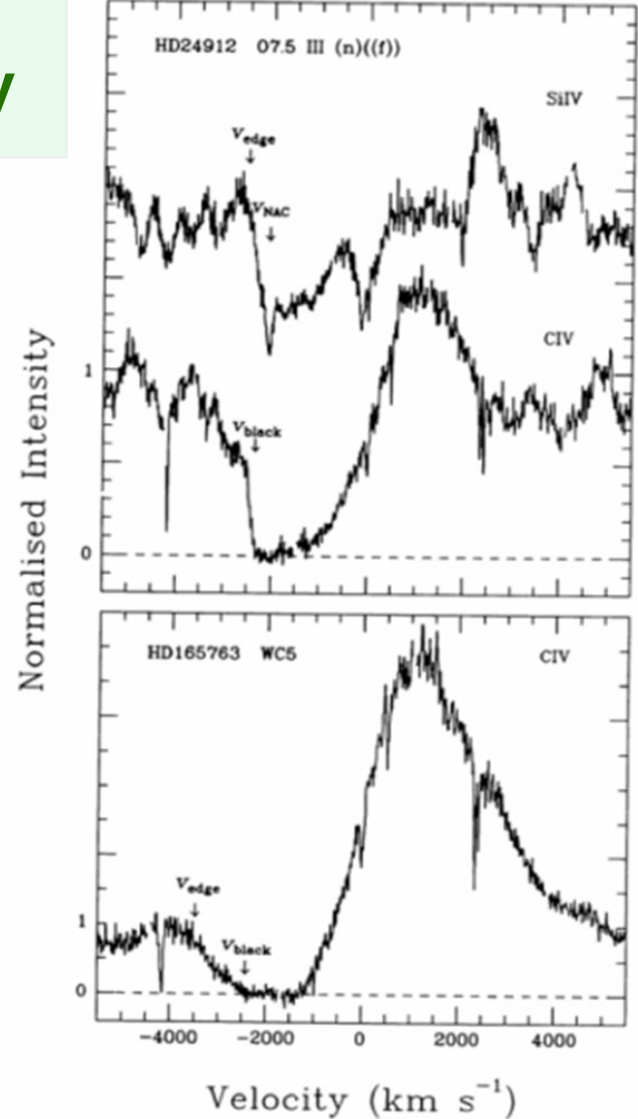


FIG. 1.—Examples of the principal stellar wind velocity measurements made on the UV resonance line profiles of O and WR stars.

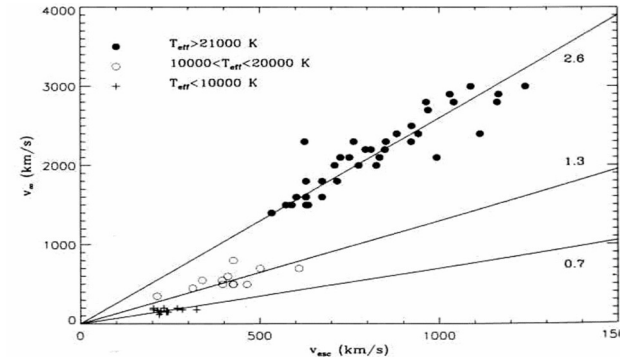
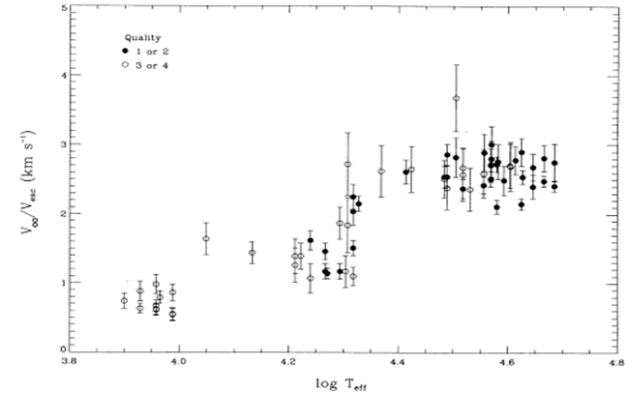
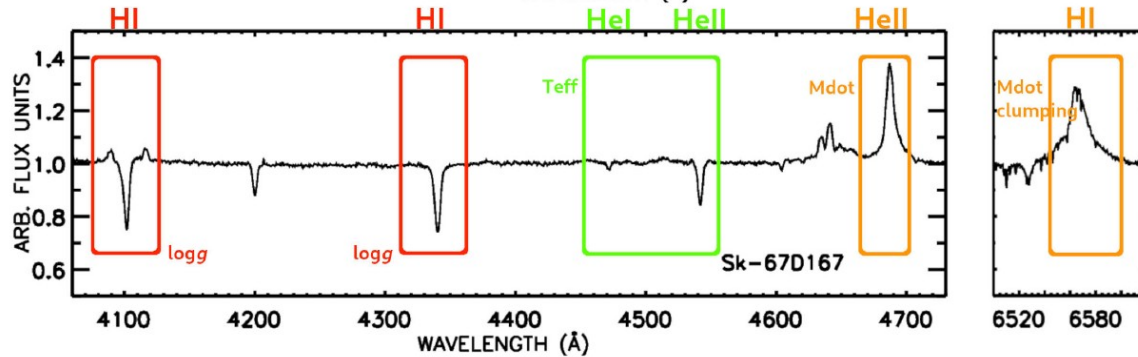
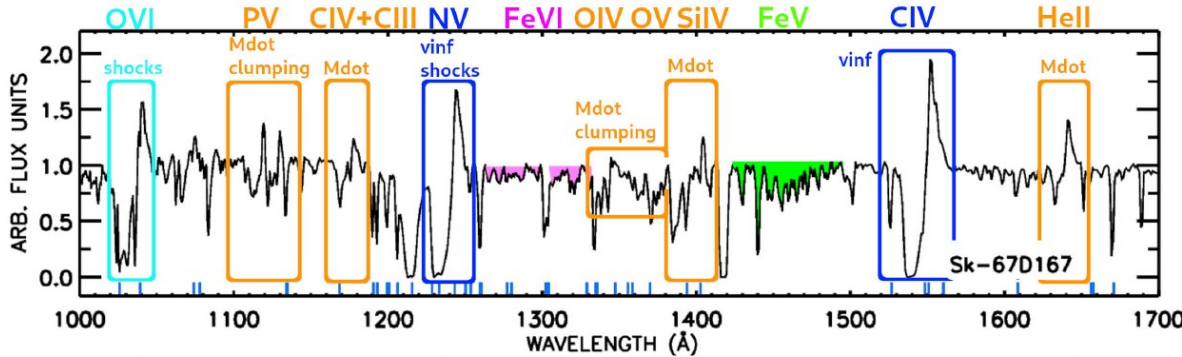
Hot Massive Stars: Terminal Velocity

!!! Only UV lines in spectra of OB-type stars have P Cyg profile

$$v_{\infty} = C(T_{\text{eff}}) \cdot v_{\text{esc}}$$

$$\begin{cases} C(T_{\text{eff}}) = 2.65, & T_{\text{eff}} \geq 21,000 \text{ K} \\ C(T_{\text{eff}}) = 1.4, & 10,000 \text{ K} < T_{\text{eff}} < 21,000 \text{ K} \\ C(T_{\text{eff}}) = 1.0, & T_{\text{eff}} \leq 10,000 \text{ K} \end{cases}$$

Kudritzki & Puls (2000)



Vink, Ulysses project (2023)

Hot Massive Stars: Mass Loss Rate

Massive stars lose a large fraction of their mass to radiation-driven winds throughout their entire life. These outflows impact both the life and death of these stars and their surroundings. Theoretical estimations of mass-loss rates is most important for stellar evolution calculations.

Radiative mass-loss rate by Vink et al. (2000)

$$\begin{aligned} \log \dot{M} = & -6.697(\pm 0.061) + 2.194(\pm 0.021) \log(L_*/10^5) \\ & -1.313(\pm 0.046) \log(M_*/30) - 1.226(\pm 0.037) \log\left(\frac{v_\infty/v_{\text{esc}}}{2}\right) \\ & + 0.933(\pm 0.064) \log(T_{\text{eff}}/40000) - 10.92(\pm 0.90) \{\log(T_{\text{eff}}/40000)\}^2 \end{aligned}$$

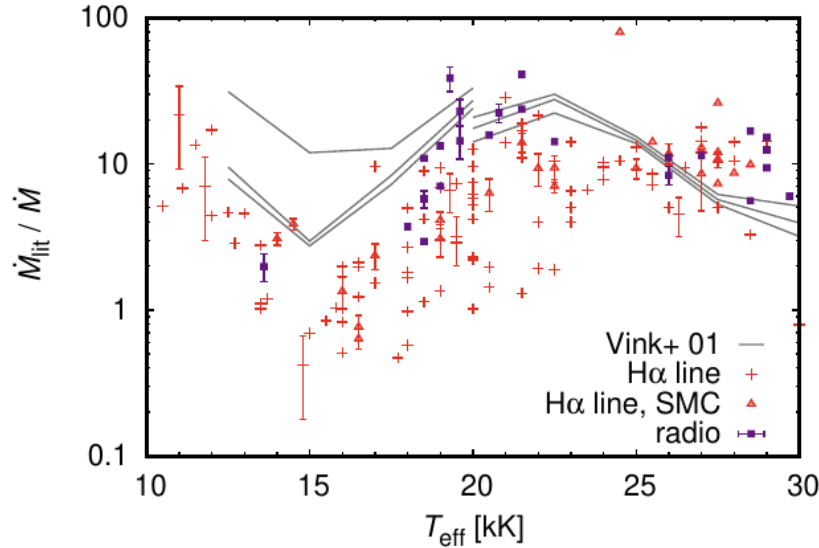
for $27\,500 < T_{\text{eff}} \leq 50\,000\text{K}$

!!! These ratios are used
in Geneva
evolutionary models

$$\begin{aligned} \log \dot{M} = & -6.688(\pm 0.080) + 2.210(\pm 0.031) \log(L_*/10^5) \\ & -1.339(\pm 0.068) \log(M_*/30) - 1.601(\pm 0.055) \log\left(\frac{v_\infty/v_{\text{esc}}}{2}\right) \\ & + 1.07(\pm 0.10) \log(T_{\text{eff}}/20000) \end{aligned}$$

for $12\,500 < T_{\text{eff}} \leq 22\,500\text{K}$

Hot Massive Stars: Mass Loss Rate

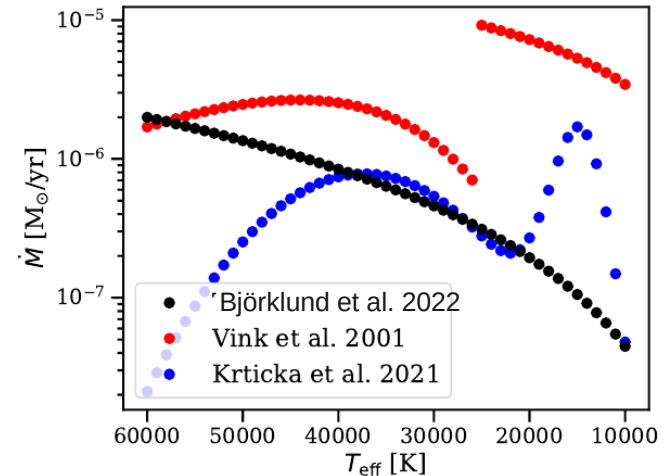


Krtićka et al. 2021

$$\log \left(\frac{\dot{M}}{1 M_{\odot} \text{yr}^{-1}} \right) = a + b \log \left(\frac{L_*}{10^6 L_{\odot}} \right) - a \log \left\{ \exp \left(-\frac{(T - T_1)^2}{\Delta T_1^2} \right) + c \exp \left(-\frac{(T - T_1)^2}{\Delta T_1^2} \right) \right\}$$

Björklund et al. 2022

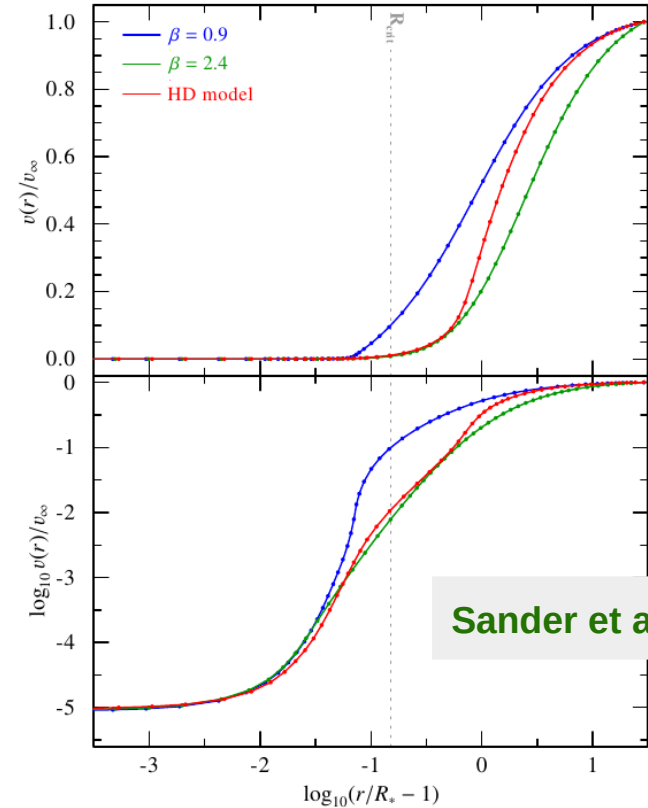
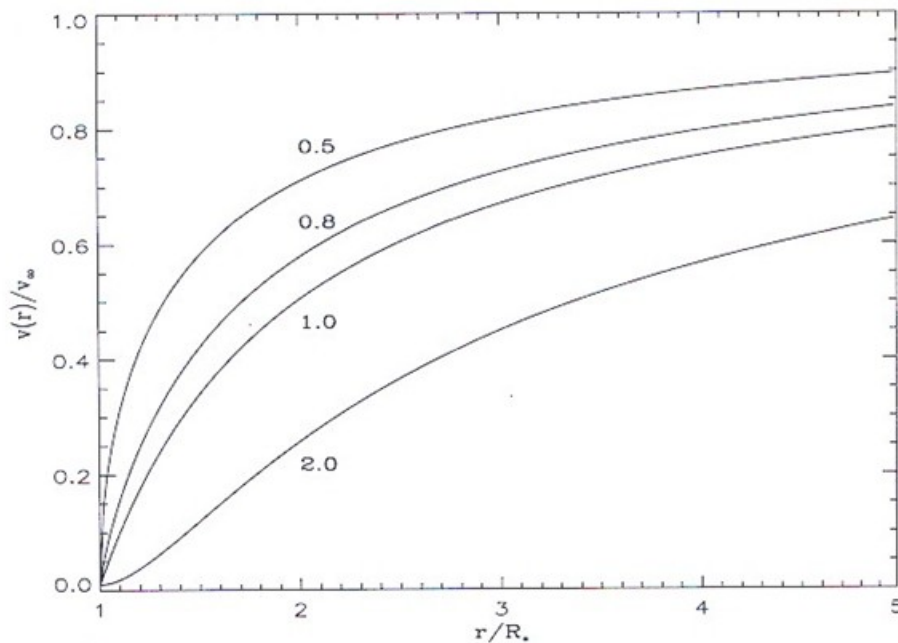
$$\log \dot{M} = -5.52 + 2.39 \log \left(\frac{L_*}{10^6 L_{\odot}} \right) - 1.48 \log \left(\frac{M_*}{45 M_{\odot}} \right) + 2.12 \log \left(\frac{T_{\text{eff}}}{4500 \text{K}} \right) + \left(0.75 - 1.87 \log \left(\frac{T_{\text{eff}}}{4500 \text{K}} \right) \right) \log \left(\frac{Z_*}{Z_{\odot}} \right)$$



Empirical Velocity Law for Hot Stars

$$v = v_{\infty} \left(1 - \frac{r_o}{r}\right)^{\beta}$$

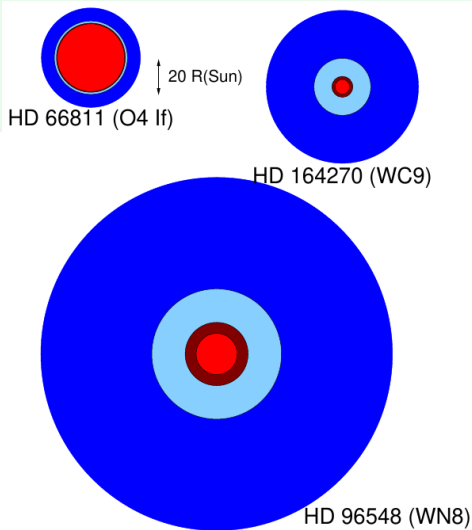
The beta velocity law



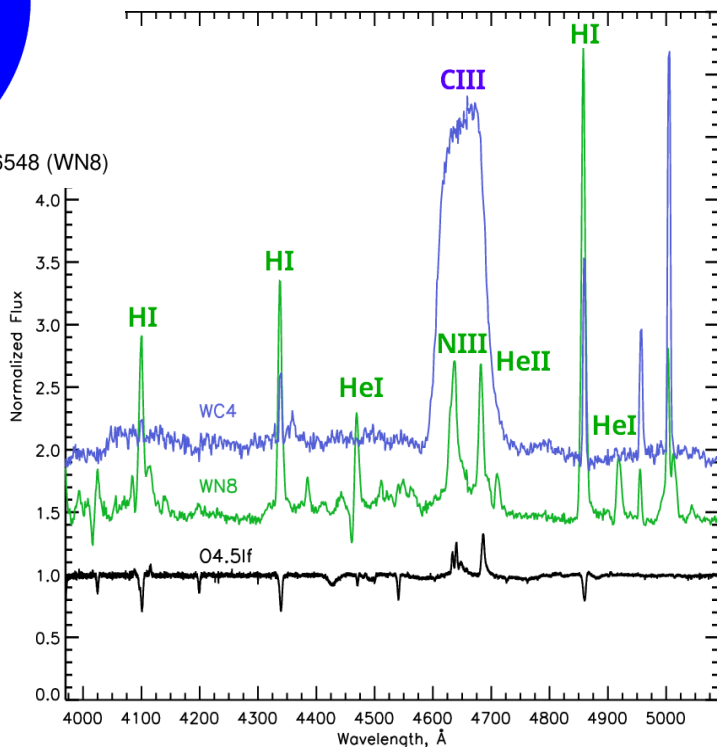
Sander et al. 2017

Hydrodynamically consistent models using a comoving-frame radiative transfer

Wolf-Rayet Stars: Line Driven Winds



Winds of WR stars are optically thick. Winds are mainly radiatively driven with iron opacities playing a critical role for acceleration of the wind and the scaling of the mass-loss rate.



Sp Type	T_* kK	$\log L / L_\odot$	$\dot{M} / M_\odot \text{yr}^{-1}$	$v_\infty / \text{km s}^{-1}$
WN 3	85	5.34	-5.3	2200
WN 4	85	5.3	-4.9	1800
WN 5	60	5.2	-5.2	1500
WN 6	70	5.2	-4.8	1800
WN 7	50	5.54	-4.8	1300
WN 8	45	5.38	-4.7	1000
WN 9	32	5.7	-4.8	700
(WO)	(150)	(5.22)	(-5.0)	(4100)
(WC 4)	(90)	(5.54)	(-4.6)	(2750)
WC 5	85	5.1	-4.9	2200
WC 6	80	5.06	-4.9	2200
WC 7	75	5.34	-4.7	2200
WC 8	65	5.14	-5.0	1700
WC 9	50	4.94	-5.0	1200

Red Supergiants: Dust Driven Winds

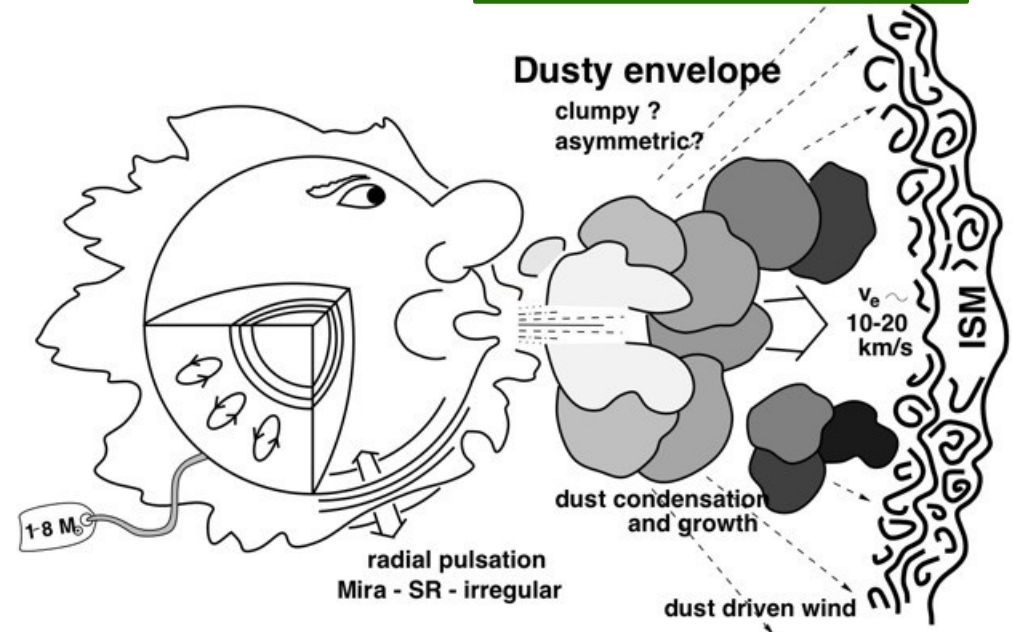
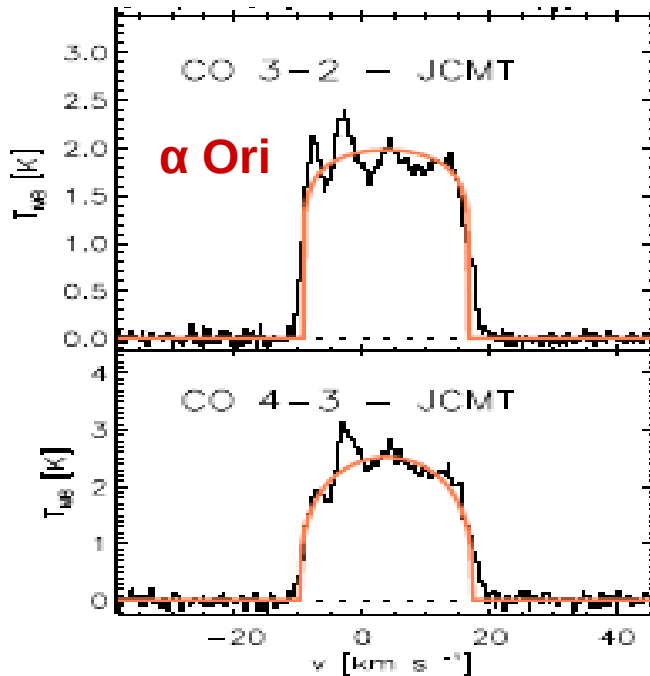
$$\dot{M}_{min} = 6.6 \times 10^{-8} \left(\frac{M_*}{M_\odot} \right)^2 \left(\frac{L_*}{10^4 L_\odot} \right)^{-1} M_\odot \text{ yr}^{-1}$$

$$\approx 10^{-7} M_\odot \text{ yr}^{-1}$$

$$\dot{M}_{max} \approx 1.1 \times 10^{-5} \left\{ \frac{\tau_{Ros}(tot)}{10} \right\} \left\{ \frac{L_*}{10^{4.5} L_\odot} \right\}^{0.5} \left\{ \frac{T_{eff}}{2500K} \right\}^{-2} M_\odot \text{ yr}^{-1}$$

$$\approx 10^{-5} M_\odot \text{ yr}^{-1}$$

$v_\infty < 50 \text{ km/s}$



Red Supergiants: Dust Driven Winds

Stars with $M^* \approx 8-30M_{\odot}$ evolve through **Red Supergiant phase**. Strong \dot{M} has important consequences for their subsequent evolution and eventual demise as core-collapse SN

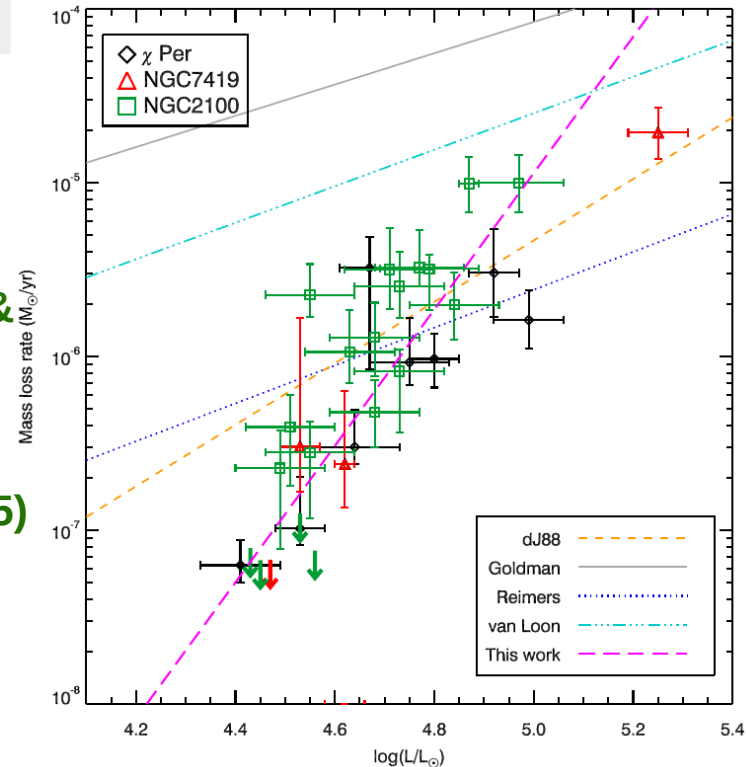
Empirical mass-loss rates for red supergiants

$$\dot{M} = 10^{-8.158} \left(\frac{L_*}{L_{\odot}} \right)^{1.769} (T_{\text{eff}})^{-1.676} \quad \text{de Jager et al. (1988)}$$

$$\dot{M} = 10^{-14.02} \left(\frac{L_*}{L_{\odot}} \right)^{1.24} \left(\frac{M_*}{M_{\odot}} \right)^{0.16} \left(\frac{R_*}{R_{\odot}} \right)^{0.81} \quad \text{Nieuwenhuijzen \& de Jager (1990)}$$

$$\dot{M} = 10^{-5.65} \left(\frac{L_*}{10^4 L_{\odot}} \right)^{1.05} \left(\frac{T_{\text{eff}}}{3500} \right)^{-6.3} \quad \text{van Loon et al. (2005)}$$

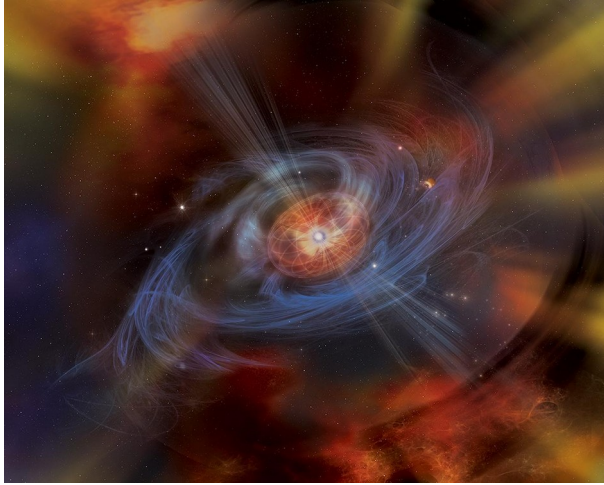
$$\dot{M} = 10^{-26.4 - 0.23 M_*/M_{\odot}} \left(\frac{L_*}{L_{\odot}} \right)^{4.8} \quad \text{Beasor et al. (2020)}$$



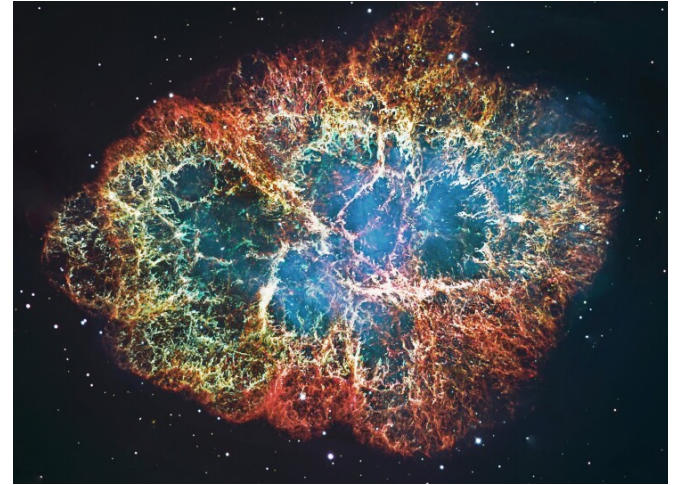
Pulsar winds

Some pulsars generate an outflowing wind of charged particles travelling at nearly the speed of light, resulting in a pulsar wind nebula around them.

Vela Pulsar

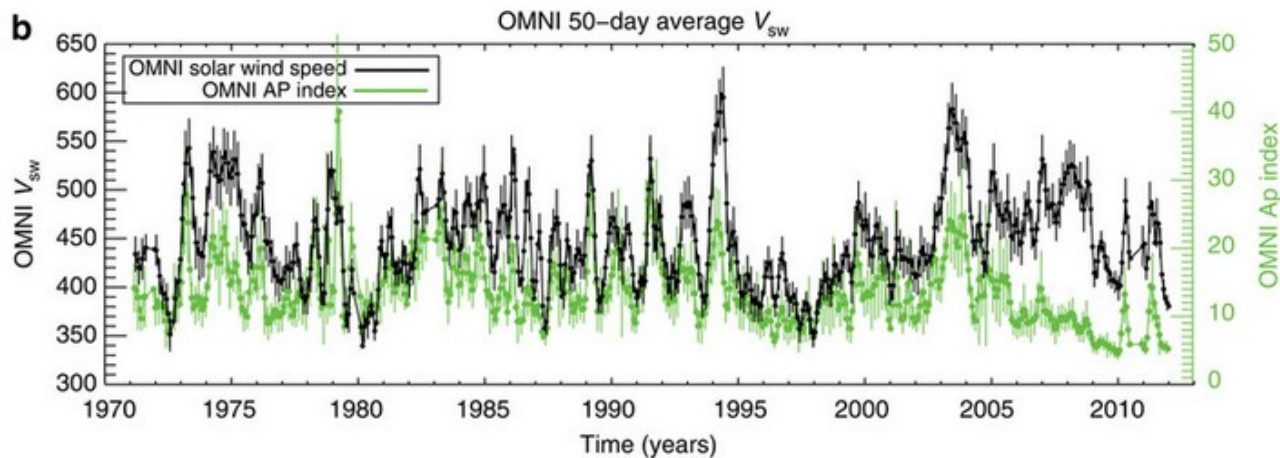
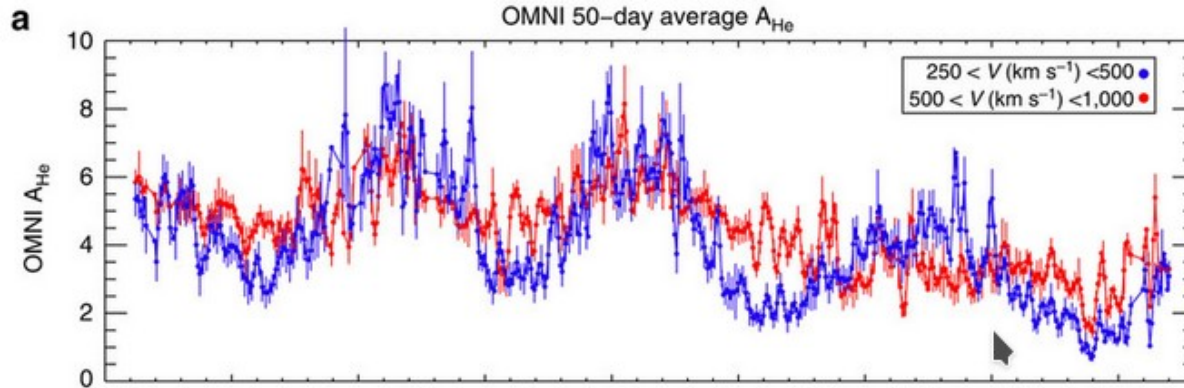


Crab Pulsar



Wind Variability: Solar Wind

Magnetic fields lead to extensive structure and variability in the solar corona and wind



Variation of solar wind and geomagnetic properties over the past four decades.

(a) Variation in 50-day running averages of the fast (red) and slow (blue) solar wind helium abundance — a proxy of plasma heating at the base of the solar wind¹⁶.

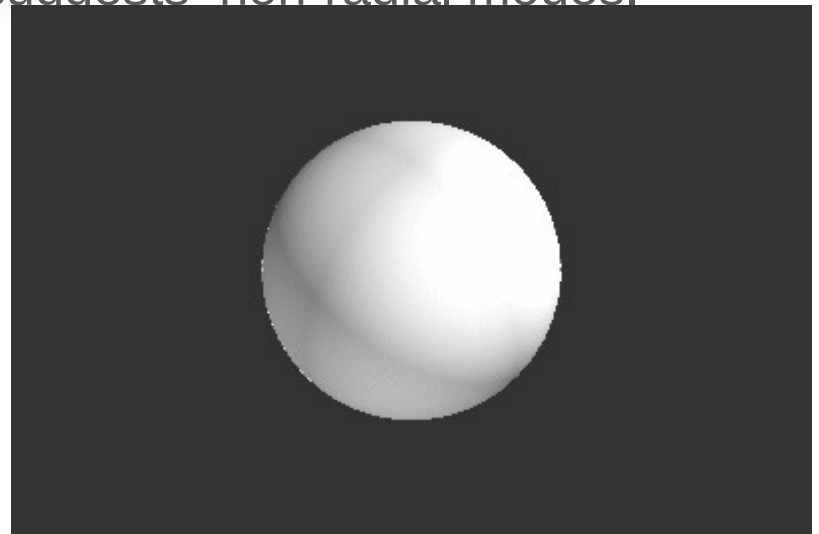
(b) Variation in the 50-day running averages of the solar wind speed (V_{sw} ; black) and geomagnetic storm Ap index (green).

McIntosh et al. 2015

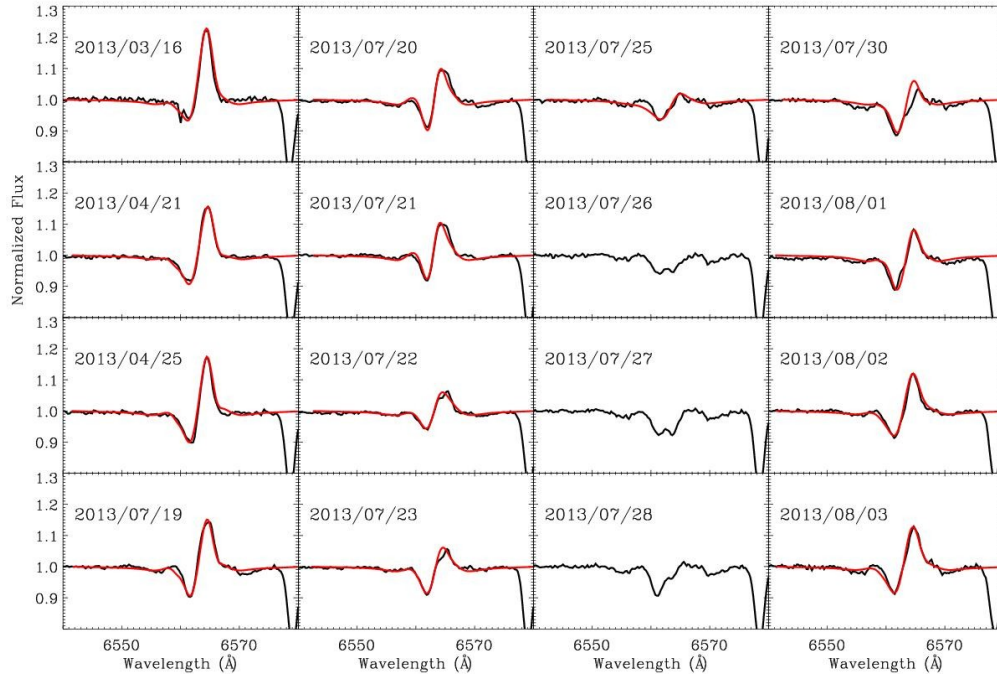
Wind Variability

Pulsations: Stellar pulsation is associated with some of the most dramatic epochs of mass loss from stars.

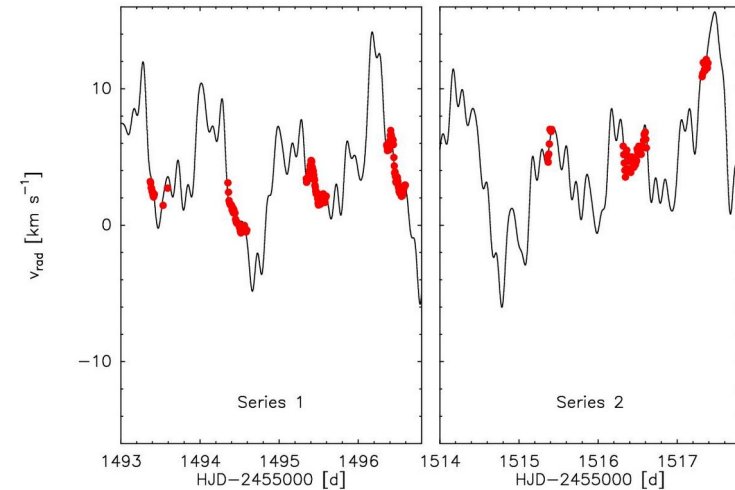
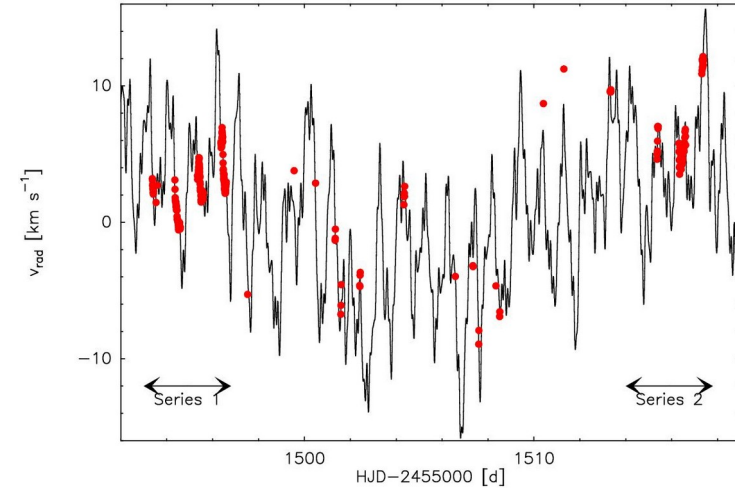
Spectral variability in an Of-type star were first detected by Vogt and Penrod (1983) and Baade, 1986). Spectroscopic and photometric changes on the time scale of some eight hours suggests non-radial modes.



Pulsations and Mass-loss Variations



55 Cyg undergoes episodes of variable mass-loss rates that change by a factor of 1.7–2 in day time scales. Kraus et al (2015) interpreted line spectral variations (from hours to 22.5 days) in terms of oscillations in p-, g-, and strange modes



Wind Variability: Discrete absorption components

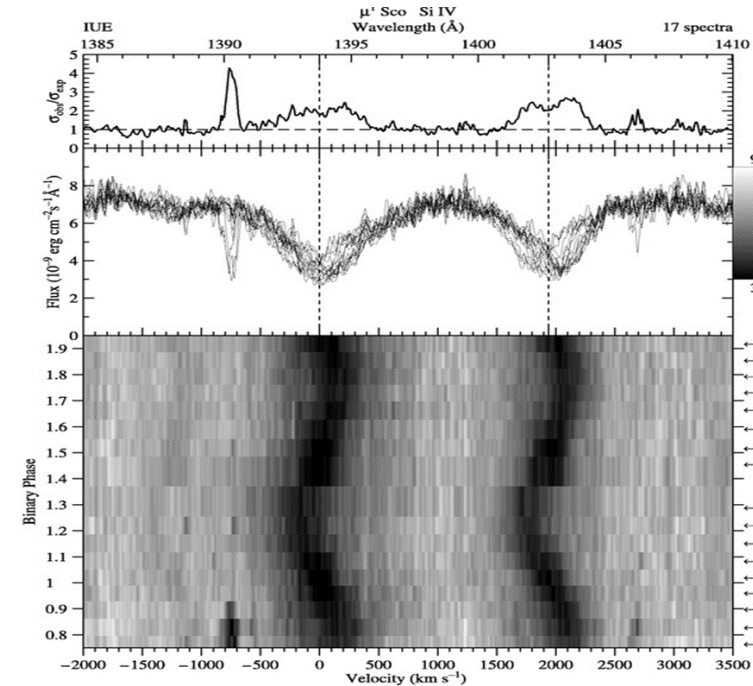
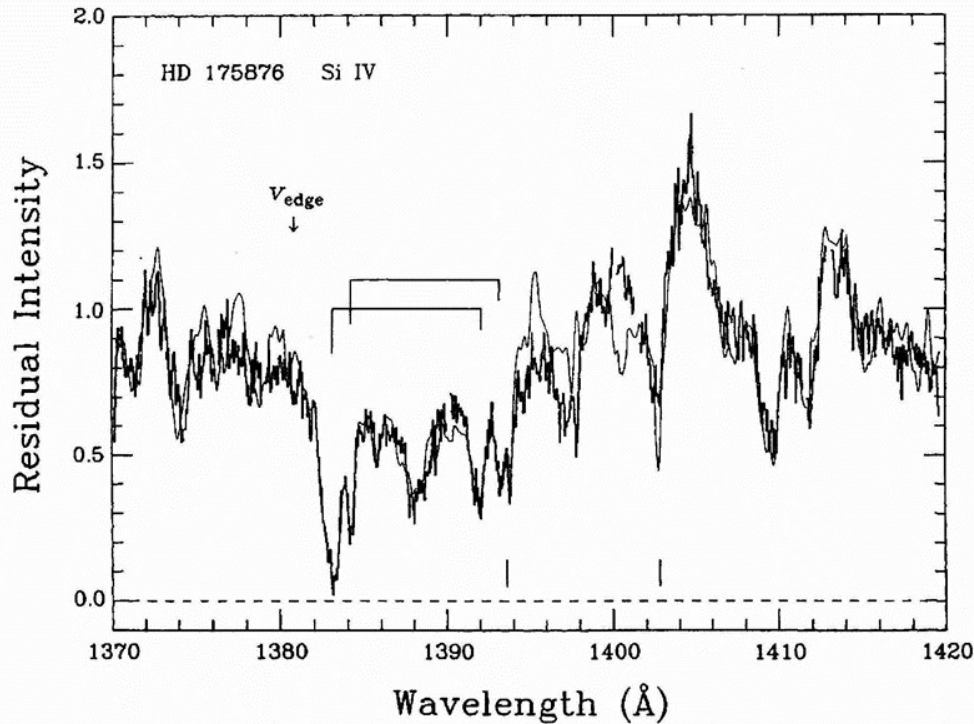


FIG. 6.—An example of a typical P Cygni profile fit (thin line), with the doublet rest wavelengths and multiple narrow absorption features marked

DACs varies in velocity and intensity
The width of the components is $300\text{-}400 \text{ km s}^{-1}$

Evolution of Discrete Absorption Components

There are few stars (OB supergiants and Be stars) where changes in non radial pulsations shows great changes in the DACs and on the H lines (Henrichs 1984).

2-spot best fit: $V_{\text{spot}} = V_{\text{rot}} / 5$
 $A_{\text{spot}} = 0.2 \quad \Phi_{\text{spot}} = 20^\circ$
 $A_{\text{spot}} = 0.08 \quad \Phi_{\text{spot}} = 30^\circ$

J Puppis IUE 1995

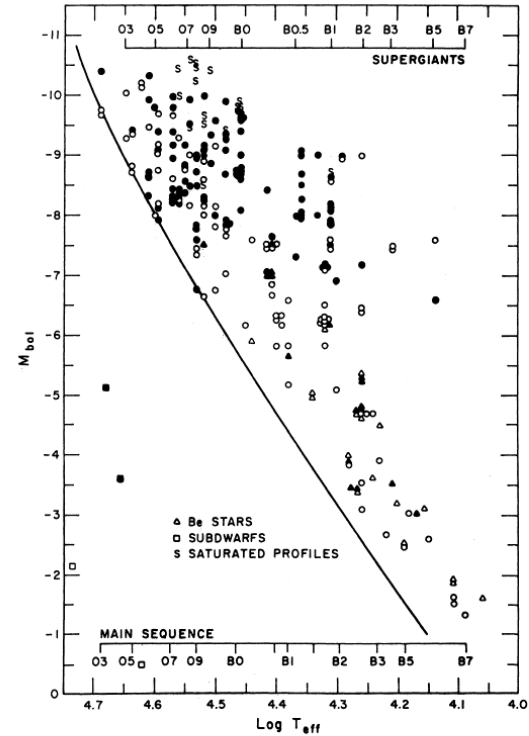
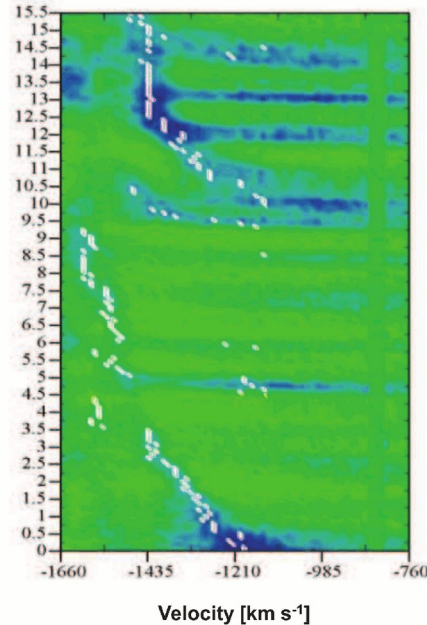
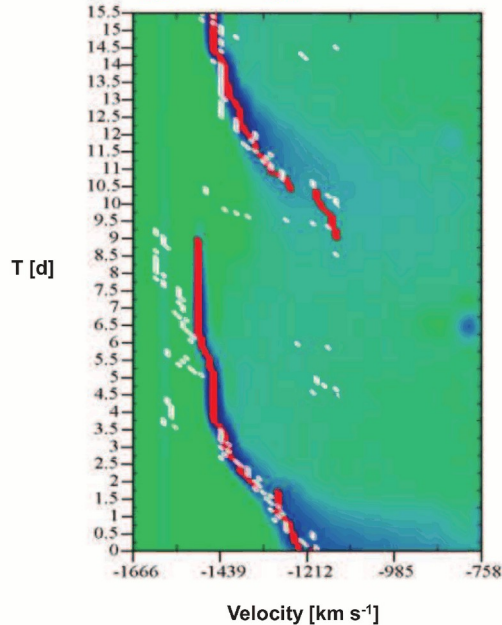


FIG. 1—A theoretical H-R diagram with the position of 110 O stars, 4 sdO stars, 96 B stars, and 31 Be stars searched for the presence of discrete absorptions in ultraviolet resonance lines of Nv, SiIV, and C IV (Henrichs and Wakker 1986). A filled symbol indicates a positive identification. Most (if not all) of the discrete absorption features are variable. An s denotes saturated P Cygni profiles, making identification impossible. One of the major conclusions from this diagram is that among the (non-supergiant) B stars below $M_{\text{bol}} = -7$, all stars that show discrete absorption features are Be stars. In some of them (ζ Oph, λ Eri, δ Cep) the variability of the discrete absorptions in the UV have been observed to be related to H α emission variability and nonradial pulsation behavior.

(1982), Howarth *et al.* (1984), and Henrichs (1984). The most complete review of models is given by Prinja and Howarth (1985). They distinguish six different categories:

velocity plateau(s), increased ionization fraction, enhanced mass column, shell ejection models, models incorporating rotation, and Lucy's multiple shock model. None of the models in the presently available form is capable of explaining all the details and features of the

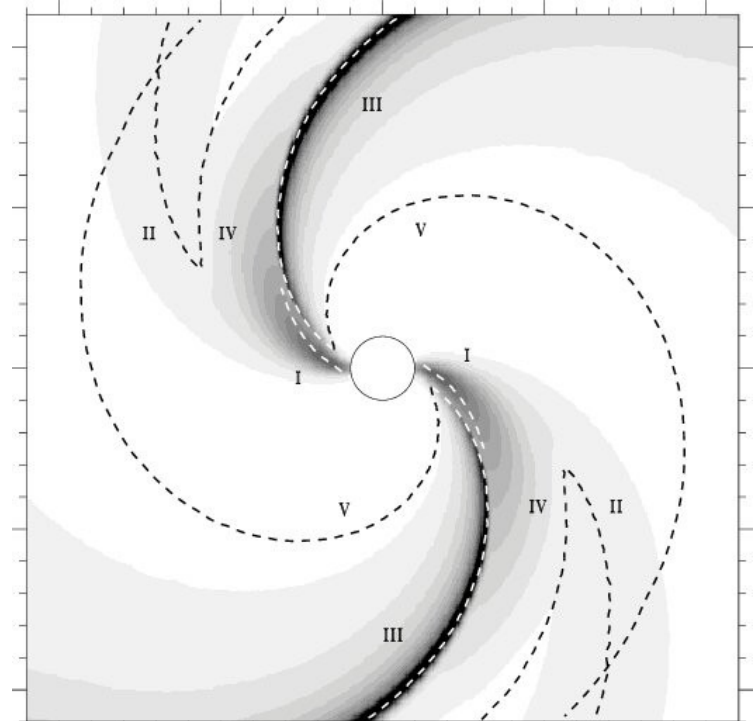
Henrichs 1986

Co-Rotating Interaction Region

Hydrodynamic models of **Co-rotating Interaction Regions (CIRs)** have been proposed to explain the observed **DAC** properties qualitatively

A corotating interaction region (CIR) is formed when a rotating star emits wind in a non-spherically symmetric manner.

Mullan (1984) developed the first model for the solar corona which does not expand in a spherically symmetric manner. Certain regions of the corona emit “**high-speed streams**” with wind speeds up to 800 km s^{-1} , while other regions emit **slower material** around $300\text{-}400 \text{ km s}^{-1}$



The CIR model of Cranmer & Owocki (1996) for the case of the Bright Spot model. I) Enhanced mass flux above the bright spot, III) is the CIR compression. According to their model, the largest relative contribution to the Sobolev optical depth (producing DACs in line profiles) comes from region V, the so-called radiative acoustic Abbott kink.

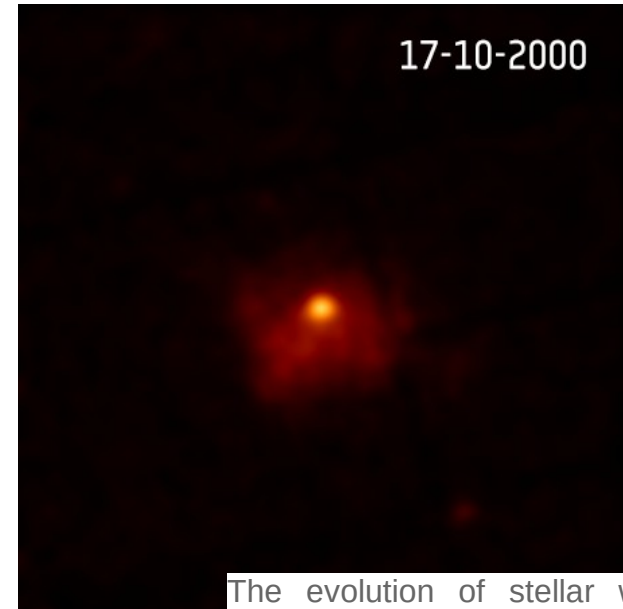
Wind-Wind Collision

HD 5980 had a major outburst on 24 October 1994 (**Eta-Carina type outburst**) discovered by Barbá & Niëmela at CASLEO Observatory (Argentina)

Nazé et al. (2007) **discovered the collision of winds** from these stars using observations made by ESA's XMM-Newton and NASA's Chandra X-ray telescopes between 2000 and 2005.

When stellar winds collide, the shocked material releases plenty of X-rays. However, if the hot matter radiates too much light, it rapidly cools, the shock becomes unstable and the X-ray emission dims.

But by 2016, the shock had relaxed and the instabilities had diminished, allowing the X-ray emission to rise eventually



The evolution of stellar winds in the binary star system HD 5980 as observed by ESA's XMM-Newton between 2000 and 2016.

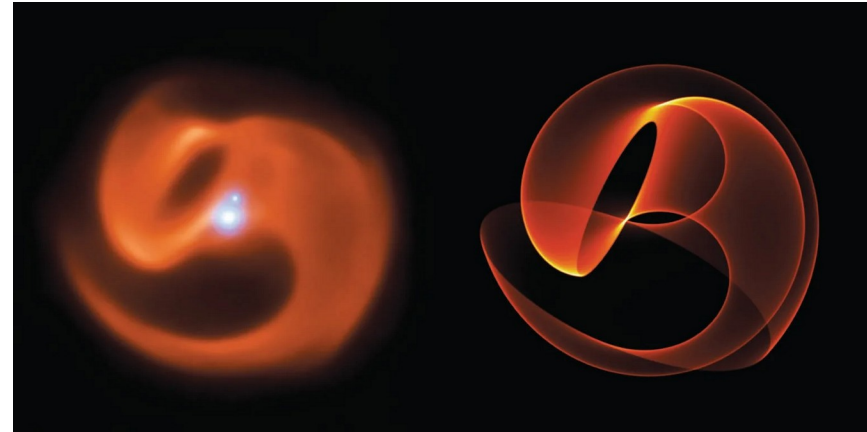
Binary Interaction and Dust Formation

Peredur Williams (1980) linked the creation of dust to the eight-year period of a binary companion co-orbiting with the Wolf-Rayet. Dust forms when the pair makes its closest approach. This colliding-wind dust mechanism requires that both stars launch powerful winds.

Ripples of dust around WR 140



An infrared image from the James Webb Space Telescope depicting 15 successive dust shells puffed out at intervals with the system's eight-year binary orbit.

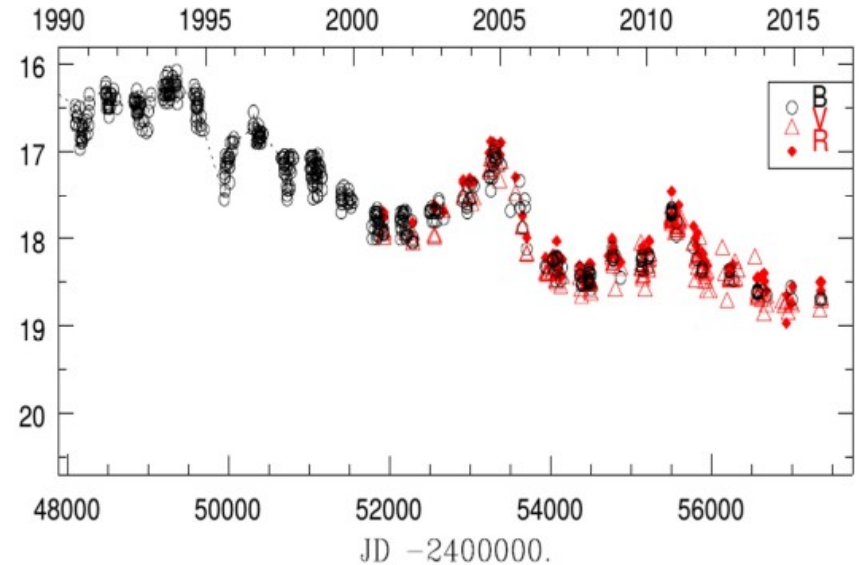
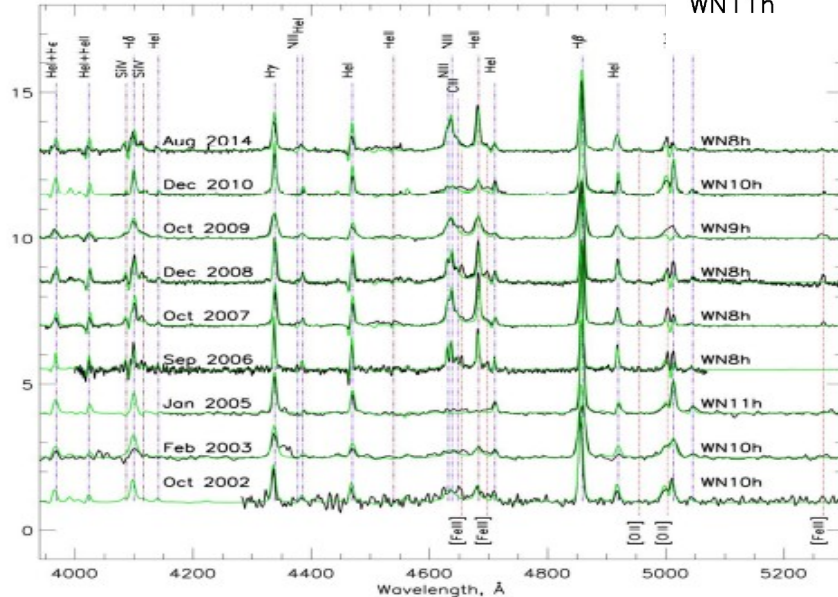
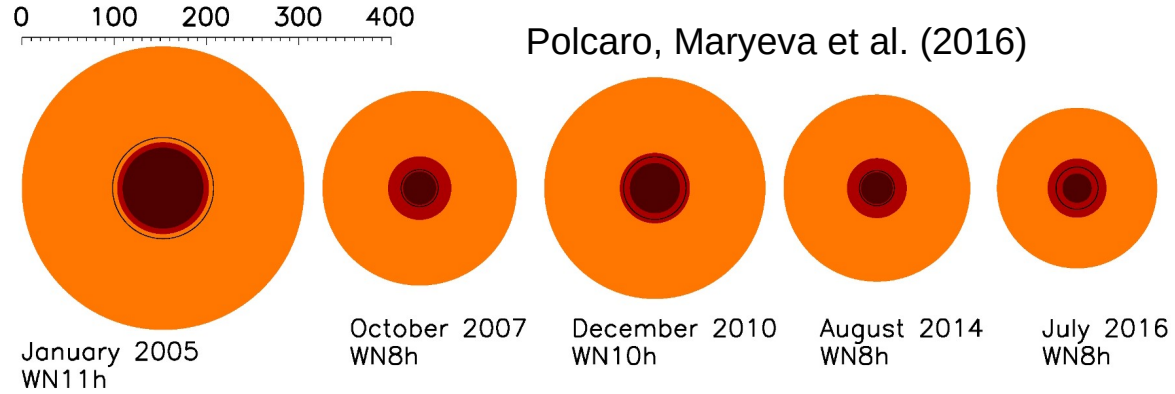


The Apep triple-star system, seen in infrared (*left*), ejects a sculpted plume of hot dust around it. A computer simulation of the dust (*right*): Credit: ESO/Callingham et al., 1999 (*left*); Yinuo Han/Peter Tuthill (*right*)

Wind Variability: Luminous Blue Variables

Romano's star (M33 galaxy)

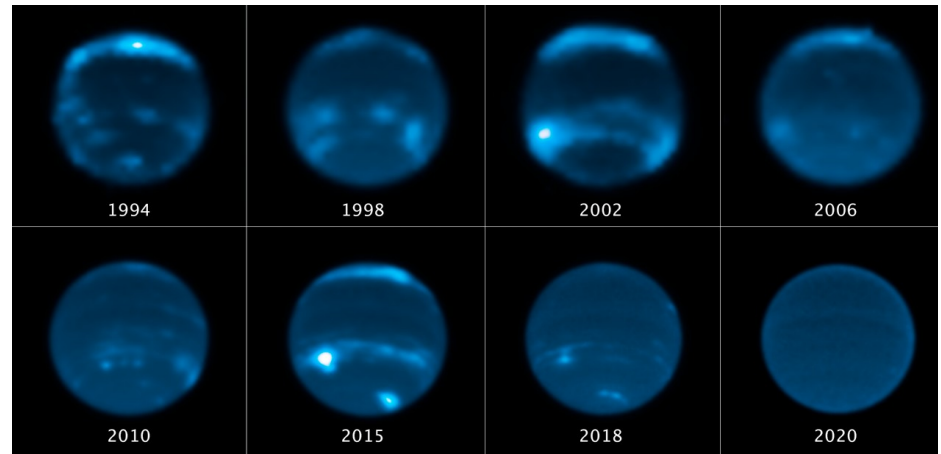
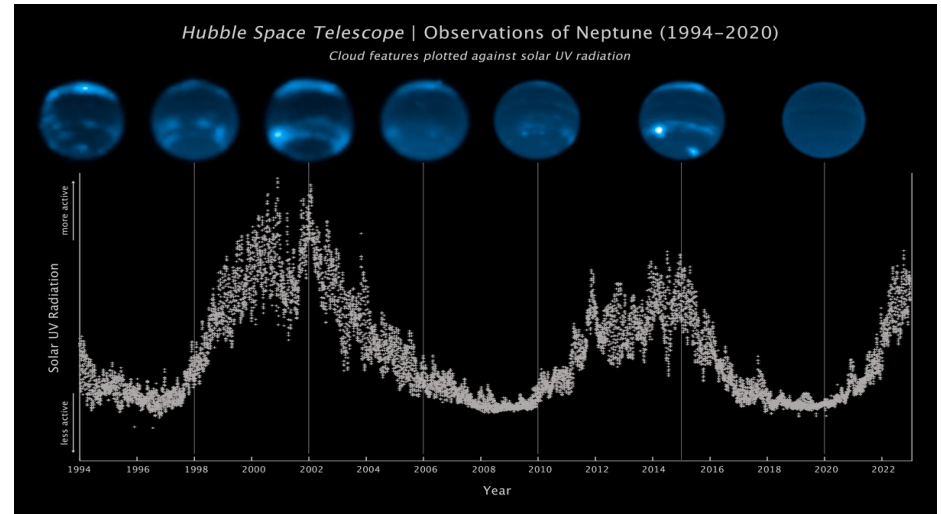
Nature of the wind significantly changes, during the eruption in 2005 the wind is much denser and slower. In the minima of brightness the wind structure is fairly similar to the one of typical WN8h (non variable) stars.



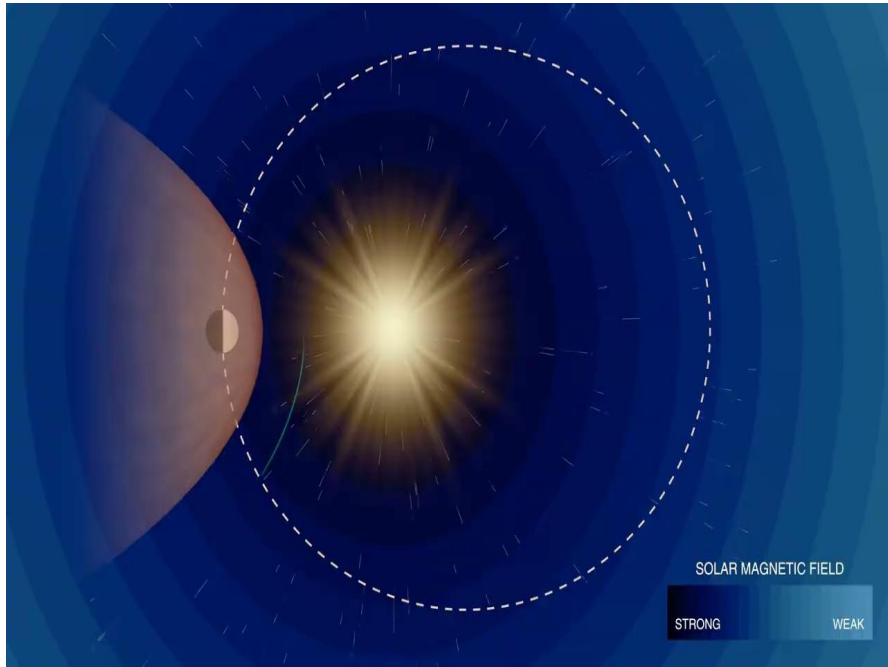
Stellar Winds Influence: Planetary Atmospheres

Earth: auroras are the result of disturbances in the magnetosphere caused by the solar wind.

Neptune: amount of cloud cover on Neptune grows increasingly following a peak in the solar cycle. The chemical changes are caused by photochemistry

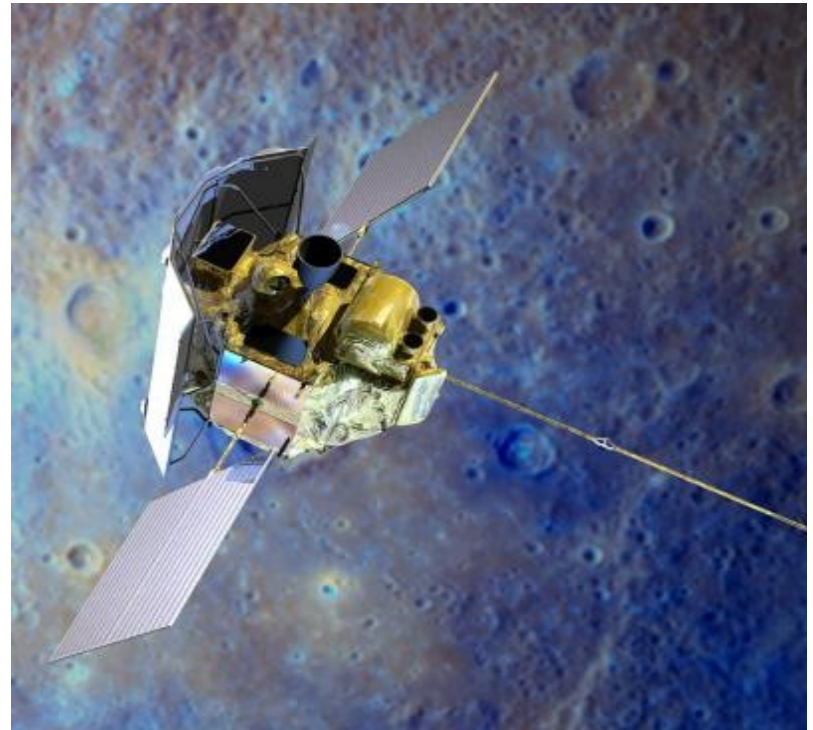


Stellar Winds Influence: Planetary Atmospheres



Ultra Low Frequency (ULF) waves rebounding from Mercury's foreshock, the turbulent area where solar wind particles collide with Mercury's magnetosphere.

Mercury provides a unique opportunity to study how the Sun's influence on a planet varies with distance.



Stellar Winds Influence: Interaction with ISM

Stellar bow shock nebulae are arcuate structures created by interaction between stellar winds and surrounding interstellar medium (ISM) where relative velocity between the two is supersonic. Shock front forms at interface of high speed stellar wind and ambient interstellar medium.

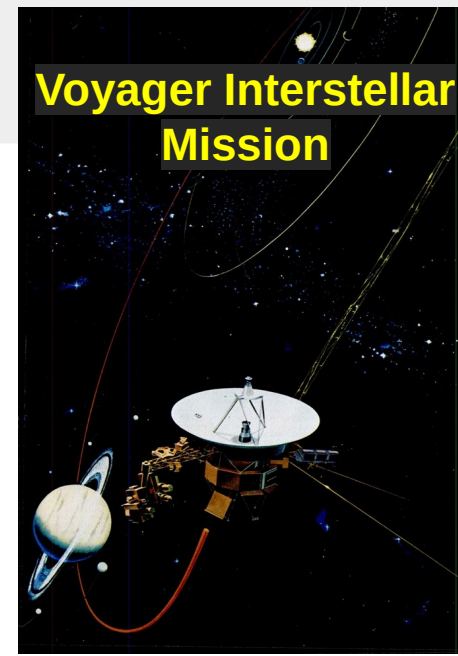
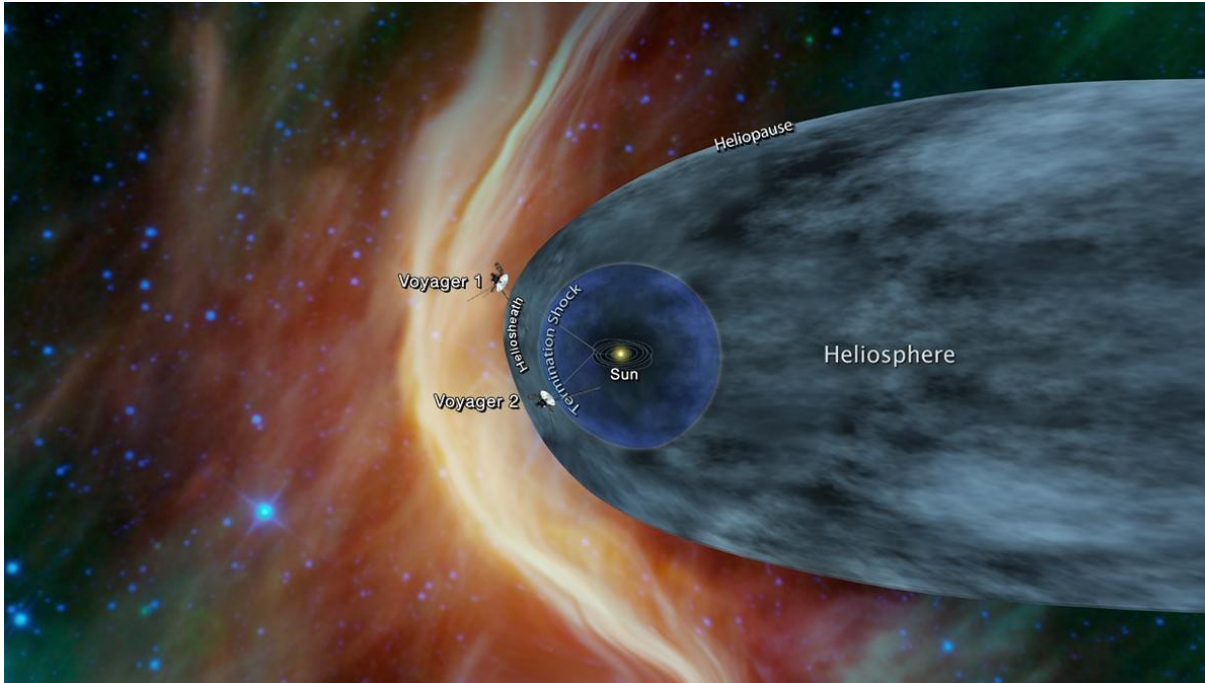
“Catalog of 709 Mid-infrared Selected Candidates”
Kobulnicky et al. (2016)



Circumstellar shells have roughly spherical shapes and are not gravitationally bound to the star core. Usually circumstellar envelopes are formed from the dense stellar wind, or they are present before the formation of the star.

Stellar Winds Influence: Interaction with ISM

- Heliosphere is not a perfect sphere, it is flattened: its southern border is closer to the Sun than its northern one.
- At the boundary of the shock wave, the temperature was higher than in the inner heliosphere, but still the difference is 10 times less than expected.

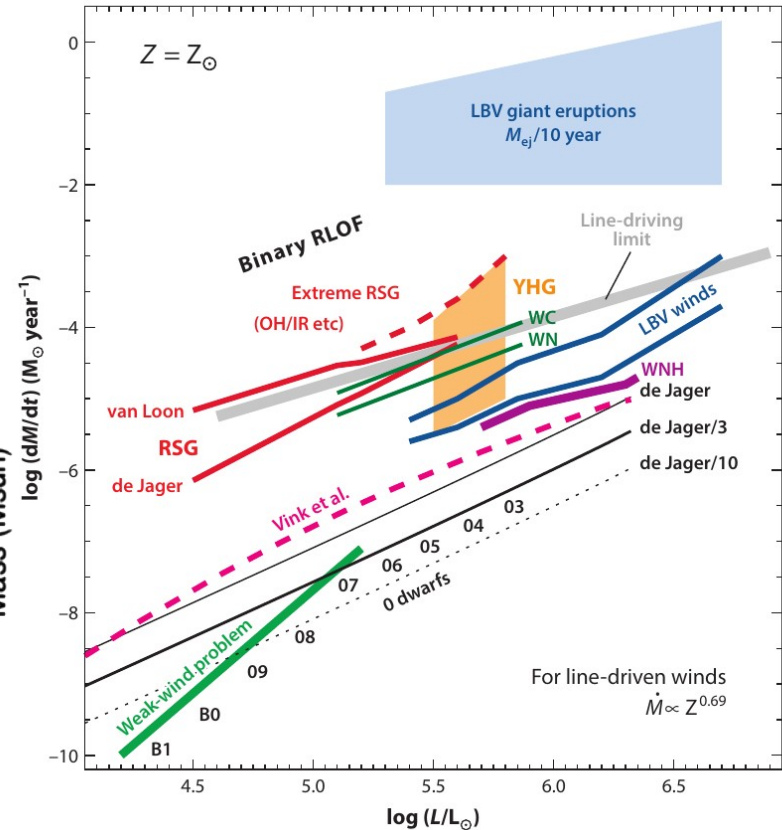
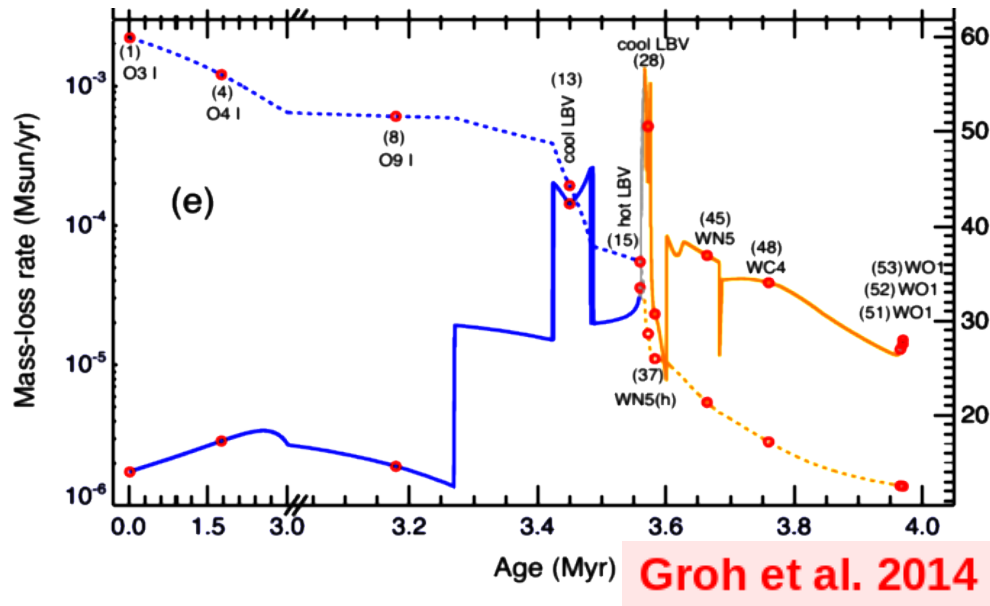


Stellar Winds Influence: Stellar evolution

\dot{M} is important ingredient for stellar evolution

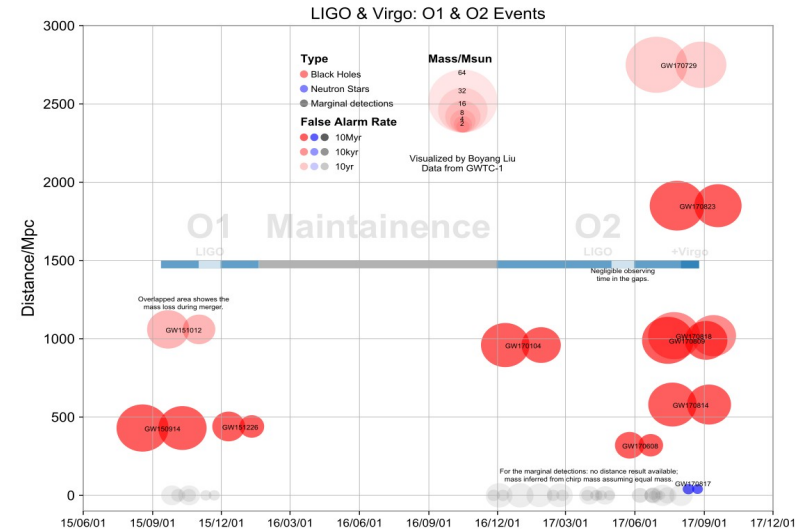
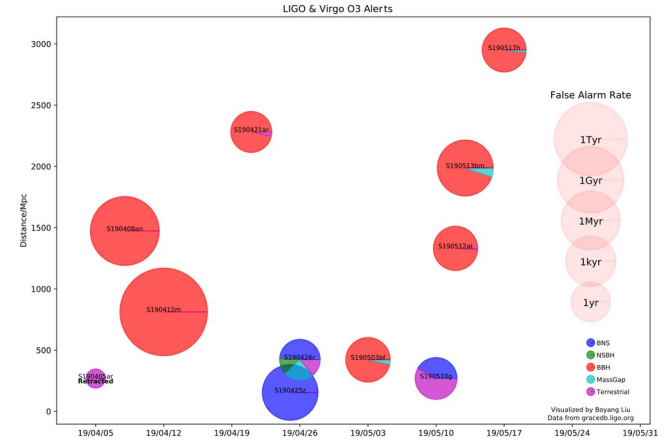
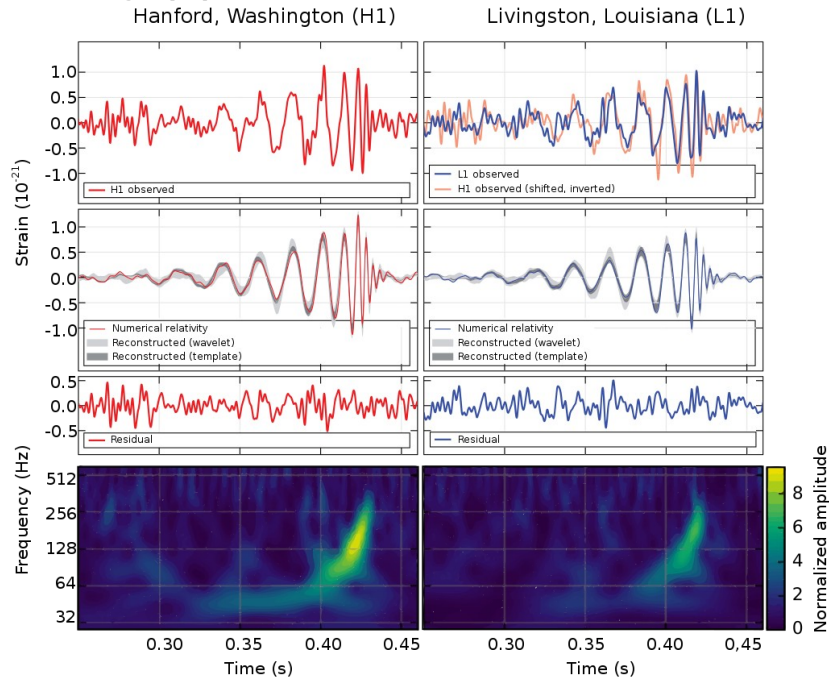
For lower-mass (**1-8 M_{sun}**) stars it defines the life time on post-AGB stage (superwind phase)

RSG (**8-30 M_{sun}**) \rightarrow it defines final pre-supernova mass & mass of compact remnant
 LBV & WR (**>30 M_{sun}**) \rightarrow



Stellar Winds Influence: Stellar evolution

Since the detectability of **gravitational waves** and along with it the significant amount of black holes (BHs) above $20 M_{\odot}$, the interest in a better understanding of the BH-mass limiting WR mass loss as a function of metallicity (Z) has increased even further



Supershells are the result of the collective influence of stars on the interstellar medium

Evolution of OB association:

- $t \approx 10^6$ - 10^7 years – stellar wind is main source of kinematic energy
- after leaving the main sequence of the most massive stars – stellar wind decreases, but appear SN explosions

Association	L_w , erg/s
Cyg OB1, OB3	$1.0 \cdot 10^{39}$
Car OB1	$8.3 \cdot 10^{38}$
Sco OB1	$1.7 \cdot 10^{38}$
Sgr OB1	$1.3 \cdot 10^{38}$
Ser OB1, OB2	$9.0 \cdot 10^{37}$
Per OB1	$3.2 \cdot 10^{37}$
Ara OB1a	$2.7 \cdot 10^{37}$



Motivation

- Derive accurate abundances, stellar and wind parameters (**Stellar Evolution**)
- Derive accurate extreme-UV ($\lambda < 912 \text{ \AA}$) radiation fields (**Nebular Photoionization**)
- Derive momentum and energy rates that winds deposit in the ISM
- Provide fundamental data for the study of starbursts (**Star Formation**)
- Better understanding of the hydrodynamics of winds (**Radiation Hydrodynamics**)
- Testbed of approximate methods that can be used in more complex geometries and inhomogeneous media (**Multi-dimensional Radiative Transfer**)
- Stellar population as function of age (**Chemical Enrichment of Galaxies**)

Bibliography

Lamers, H & Cassinelli, J., 1999 “**Introduction to Stellar Winds**” Cambridge University press.

Puls, J., Vink, J. S. Najarro, F., 2008 “**Mass loss from hot massive stars**”, A&ARv, 16, 209

Smith, N, 2014, “**Mass Loss: Its Effect on the Evolution and Fate of High-Mass Stars**” Annu. Rev. Astron. Astrophys. 2014. 52:487–528

***Thank you for
attention!***

***Thank you for
attention!***

